DRY WASHING OF ETHANOLIC BIODIESEL THROUGH ADSORPTION PROCESSES USING ADSORBENTS OBTAINED FROM WALNUT SHELL

João Vitor Fabian

Thesis presented to the

Escola Superior de Tecnologia e Gestão of the Instituto Politécnico de Bragança

to obtain the Master´s Degree in ***Chemical Engineering***

within the scope of the double diploma with the

Universidade Tecnológica Federal do Paraná

Supervisors

Ana Maria Queiroz

António Ribeiro

Paulo Brito

Ticiane Pokriwieck

BRAGANÇA

May, 2024

AGRADECIMENTOS

Agradeço primeiramente a Universidade Tecnológica Federal do Paraná (UTFPR), Campus Francisco Beltrão e ao Instituto Politécnico de Bragança (IPB) pela oportunidade de realizar essa tese de mestrado e pela oportunidade única que com certeza contribuiu muito para meu desenvolvimento pessoal e também profissional. Também aos professores da UTFPR que me apoiaram, acreditaram em mim e tiveram um impacto positivo não apenas no lado acadêmico, mas também pessoal: Professor Doutor André Zuber e Professor Doutor Douglas Nicolin.

Agradeço também aos meus professores orientadores do IPB e da UTFPR: Professora Doutora Ana Maria Queiroz, Professor Doutor Paulo Brito, Professor Doutor António Ribeiro e Professora Doutora Ticiane Sauer Prokriwieck, que sempre estiveram presentes quando necessitado e me incentivaram desde o começo deste trabalho. Obrigado por todo conhecimento compartilhado e ajuda.

Agradeço a engenheira Maria João pela paciência e sempre pela cordialidade do dia-a-dia, além de ser uma excelente profissional, é uma inspiração em como levar a vida.

Um agradecimento especial aos meus amigos: Vinicius Mai, Maísa Saldanha Pinheiro, Camila Groxko Smolich, Miriam Domingues, Carlos André Dalberto, João Pedro Lopes, Giovana Cenci, José Eduardo Pagliosa, Luis Fernando Wolker, Adam Rotava Herget, Arthur Cantu, Gustavo Rigo de Mello, Maria Fernanda Tonelli Prado e Marina Orlandini por todos os dias compartilhados, risadas e conversas. Com certeza a experiência foi mais fácil com a presença de vocês.

Aos meus colegas de laboratório: Lariane, Rafaela, Tairone, Caio, Maria, Gabriel e Eduardo por toda a ajuda sempre que necessária. Meu sincero muito obrigado.

Por último, mas não menos importante, um agradecimento a minha família por me ajudar de todos os jeitos possíveis nos tempos mais difíceis e sempre se fazer presente em todos os momentos de minha vida. Rosangela Maria Dal Piva, Eloi Gilberto Fabian, Ana Carolina Fabian, Ana Maria Dal Piva, Ivo Dal Piva, Arthur Fabian Casagrande, Maria Eduarda Fabian, Isadora Fernanda Fabian, Eloir Carlos Fabian, Fladimiria Martins Pedro e Marcos Paulo Casagrande. Eu amo vocês.

Meu sincero obrigado a todos!

ABSTRACT

Renewable energy sources present a viable and sustainable solution to the escalating global demand for clean energy. Within this context, biodiesel emerges as a prominent alternative to conventional petroleum-based fuels, with alkaline transesterification constituting the primary method of production. Subsequent to its production, biodiesel needs purification prior to its utilization in conventional engines. Among the prevailing purification techniques, "wet washing" holds prominence, despite its substantial water consumption. Conversely, an alternative purification methodology, namely "dry washing," leverages adsorption processes, offering advantages such as reduced water usage, accelerated purification kinetics, and less effluent generation. In the present investigation, biodiesel was synthesized using waste cooking oil via the ethanol route, employing a molar ratio of 1:7.5 oil to alcohol. Three activated carbons were prepared from walnut shells using different activation methodologies. These methods comprised two chemical activations, one using phosphoric acid and the other using sodium hydroxide, and a physical activation process. Surface area analyses revealed values of 426.66 m^2/g, 2.695 m^2/g, and 345.69 m^2/g for the acid, basic and physical activated carbons, respectively. Adsorption studies, including kinetics and isotherm experiments, were conducted across three temperatures: 25°C, 35°C, and 45°C. Subsequently, isotherm studies were performed at optimal temperatures determined from the kinetic assessments. Remarkably, the activated carbon prepared via phosphoric acid activation demonstrated superior removal efficiency with the increase of temperature, indicative of a negative activation energy. Notably, only the material activated via phosphoric acid allowed the 0.02% (w/w) glycerol content limit fixed by both the European EN14214 and the American ASTM D6751 standards. These findings underscore the efficacy of walnut shell-derived activated carbons in providing a viable alternative to the conventional wet washing method, thereby mitigating water wastage, and promoting a greener and more sustainable biodiesel production process.

Keywords: Adsorption, Dry Washing, Transesterification, Activated Carbon, Renewable Energy.

RESUMO

As fontes de energia renovável apresentam uma solução viável e sustentável para a crescente demanda global por energia limpa. Dentro deste contexto, o biodiesel surge como uma alternativa proeminente aos combustíveis convencionais à base de petróleo, com a transesterificação alcalina constituindo o método primário de produção. Após sua produção, o biodiesel necessita de purificação antes de ser utilizado em motores convencionais. Entre as técnicas de purificação predominantes, a "lavagem úmida" tem destaque, embora seu consumo substancial de água. Ao contrário, uma metodologia de purificação alternativa, denominada "lavagem a seco", utiliza processos de adsorção, oferecendo vantagens como redução do consumo de água, aceleração da cinética de purificação e diminuição da geração de efluentes. Na presente investigação, o biodiesel foi sintetizado utilizando óleo de cozinha residual via rota do etanol, empregando uma relação molar de 1:7.5 de óleo para álcool. Três carvões ativados distintos foram preparados utilizando diferentes metodologias de ativação envolvendo casca de noz. Estes métodos compreenderam duas ativações químicas, uma utilizando ácido fosfórico e a outra hidróxido de sódio, juntamente com um processo de ativação física. As análises de área de superfície revelaram valores respectivos de 426.66 m²/g, 2.695 m²/g e 345.69 m²/g para os carvões ativados. Estudos abrangentes de adsorção, incluindo análises de cinética e isotermas, foram conduzidos em três temperaturas designadas: 25°C, 35°C e 45°C. Posteriormente, investigações de isotermas foram realizadas em temperaturas ótimas determinadas a partir das avaliações cinéticas. Notavelmente, o carvão ativado preparado via ativação com ácido fosfórico demonstrou eficiência de remoção superior com o aumento da temperatura, indicativo de uma energia de ativação negativa. Apenas o carvão ativado via ácido fosfórico atendeu ao rigoroso limite de 0.02% (m/m) exigido tanto pela norma europeia EN14214 quanto pela norma americana ASTM D6751.

Palavras-chave: Adsorção, Lavagem a Seco, Transesterificação, Carvão Ativado, Energia Renovável.

TABLE OF CONTENTS

LIST OF FIGURES

LIST OF TABLES

NOMENCLATURE

Acronyms

AC	Activated Carbon
AAC	Acid Activated Carbon
BAC	Basic Activated Carbon
FABE	Fatty acid butyl ester
FAEE	Fatty acid ethyl ester
FAME	Fatty acid methyl ester
FAPE	Fatty acid propyl ester
FFA	Free fatty acid
IPD	Intra Particle Difusion
PAC	Physical Activate Carbon
WCO	Waste Cooking Oil

Symbols

C	Constant related to diffusion resistance ($\frac{mg}{g}$)
k_d	Intraparticle diffusion constant ($\frac{mg}{g.min^{0.5}}$)
k_1	First-order rate constant (min^{-1})
k_2	Second-order rate constant ($\frac{g}{mg.min}$)
q_e	Amount of solute adsorbed per weight unit of adsorbent at the equilibrium ($\frac{mg}{g}$)
q_t	Amount of solute adsorbed per weight unit of adsorbent in t ($\frac{mg}{g}$)
T	Time of adsorption (min)

Greek Symbols

α	Initial adsorption rate ($\frac{g}{mg.min}$)
β	Desorption constant ($\frac{mg}{g}$)

1. INTRODUCTION

The necessity of exploring new renewable fuel sources is closely tied to the desire to minimize reliance on fossil fuels and the environmental consequences of their usage. Renewable energy sources, such as biodiesel, offer a viable alternative for meeting this need. Biodiesel can be made from sustainable raw sources such as vegetable oils and animal fats and has similar properties to traditional diesel, allowing it to be utilized in diesel engines without modification. Furthermore, biodiesel is less polluting than conventional diesel, emitting fewer greenhouse gases and pollutants into the atmosphere. As a result, research and development of new renewable fuel sources, such as biodiesel, are critical to ensuring energy security, reducing reliance on fossil fuels, and promoting environmental sustainability [1].

This study continues the work of Garção [2] and Lamino Camilo [3], who investigated the effectiveness of dry washing with activated carbon in meeting the European standard for allowable glycerol content in biodiesel. Garção utilized cork, a readily available biomass waste in Portugal, as her source material and conducted both physical activation and basic chemical activation on the cork to produce two types of activated carbons. It was observed that the chemically activated carbons demonstrated superior adsorption capacities compared to the physically activated ones. Furthermore, the author found that ground cork yielded better results than merely physically activated carbon.

This work aimed to extend research by employing walnut shells, another abundant biomass waste in Portugal. We investigated both physical and chemical activation methods, using acid and base treatments, to evaluate their effectiveness in glycerol adsorption from biodiesel. The main goal of this work was the assessment of the use of natural adsorbents derived from walnut shell in the purification of biodiesel through glycerol removal. The project characterized and synthesized activated carbons via chemical and physical activation using various compounds. Adsorption tests were performed to evaluate the capacity of these materials for adsorption, with the primary goal of removing glycerol contaminants from the biodiesel produced, focusing on glycerol contamination due to its negative impact on combustion engines, which is a major issue for its application. As a result, the aim of this study was to

evaluate the production and purification of biodiesel using waste cooking oil as raw material in order to redirect its disposal toward this application.

Similarly, Lamino Camilo research followed the same methodology as Garção's but using olive stone as the biomass source. Lamino Camilo prepared five types of activated carbons: one physically activated, two chemically activated with a base, one chemically activated with an acid, and another activated with salt. His findings revealed that the salt-activated and physically activated carbons were the most effective in glycerol removal.

In Chapter 2, a comprehensive literature review was conducted on studies comparing diesel and biodiesel, focusing on the transesterification and esterification reactions involved in biodiesel production. This chapter also included a review of the various catalysts used in the production of biodiesel.

Chapter 3 delved into the adsorption process, examining which biomasses had been utilized for dry washing techniques and the types of activated carbons employed. This chapter also presented the standards that this work aimed to achieve, along with the kinetic and isotherm equations that underpinned the study.

In Chapter 4, the methodologies used for the characterization of activated carbons and the adsorption processes were detailed. This included descriptions of the procedures and techniques applied during the experimental phase.

Chapter 5 presented the results of the analyses described in Chapter 4. This section discussed the findings in detail and explored their implications.

Finally, Chapter 6 provided the conclusions of the study, summarizing the key findings and suggesting potential directions for future research.

2. BIODIESEL

Biofuels play a crucial role in the transition towards a more sustainable energy system. Biodiesel, in particular, is a renewable fuel made from sources such as used cooking oil and soybeans, and has a significantly lower environmental impact compared to traditional fossil fuels. It produces fewer greenhouse gas emissions and helps to reduce dependence on foreign oil. However, the challenge of scaling up production and ensuring long-term sustainability remains. Despite these challenges, biodiesel has the potential to be a game-changer in the fight against climate change and the transition towards a more sustainable future. This topic will discuss biodiesel production, its comparison to fossil diesel, and the catalysts that can be used for biodiesel production.

2.1 Comparison between diesel and biodiesel

Biodiesel has one of the most significant advantages among biofuels due to its comparable calorific value to fossil diesel as shown in the table 1, which does not significantly reduce engine performance. However, the pour point of biodiesel, which affects its flow characteristics inside the engine, is an important factor to consider. The pour point of biodiesel varies from -15°C to 10°C depending on the raw material used in its production, making its use impractical. The pour point of fossil diesel, on the other hand, ranges from -35°C to -15°C, providing a safer usage interval. It is critical to investigate the pour point of biodiesel produced from various raw materials in order to determine the best feedstock for its production and ensure its viability as a sustainable alternative [2].

Table 1. Comparison of some characteristics of biodiesel and diesel.

Fuel Property	Biodiesel	Diesel	Units
Fuel standard	ASTM D6751	ASTM D975	
Kinematic viscosity 40°C	1.9 – 6.0	1.3 – 4.1	$mm^2.s^{-1}$
Density	0.86 – 0.9	0.85	g/cm^{-2}
Flash point	130 – 170	60 – 80	°C
Pour point	-15 to 10	-35 to -15	°C
Heating value	34.4 – 45	42 – 45	$MJ.kg^{-1}$

Source: [2]

It is worth noting that the average calorific value of the ASTM D6751 biodiesel is slightly lower than diesel, but it is still comparable. Another important consideration is that biodiesel has a higher viscosity, which may affect its flowability in the engine.

It is important to emphasize the effect of sulfur content on fuel combustion. Given the lower sulfur content of biodiesel, a comparison with fossil diesel is relevant in this context. According to [3] biodiesel has a higher oxygen content and a lower carbon content, which allows for complete combustion and cleaner combustion. Furthermore, compared to biodiesel, fossil diesel has a higher sulfur content, indicating a dirtier combustion. According to the findings, biodiesel emits 38.66% fewer particulate pollutants than petroleum-derived diesel.

2.1 Biodiesel production

Biodiesel is a renewable fuel that can be derived from plants, algae, animal fats, and waste cooking oils. The use of these sources contributes to less reliance on fossil fuels and lower greenhouse gas emissions. Transesterification and esterification are two major biodiesel production processes. This paper provides an overview of the various biodiesel sources and production processes. Each source and process's advantages and disadvantages are discussed, as well as the potential for future research and development in this field [4].

2.2.1 Esterification

Esterification is a chemical reaction that occurs when an acid and an alcohol combine to form an ester and water. The fatty acids found in vegetable oils or animal fats are combined with an alcohol, usually methanol or ethanol, in the presence of an acidic catalyst such as sulfuric acid or hydrochloric acid to produce biodiesel esters. The fatty acids react with the alcohol to form the ester and water as a byproduct during the esterification reaction. The fatty acids are converted into esters, which can be used as a renewable fuel in this process [6].

The esterification process has gained popularity as an alternative route for biodiesel production, particularly when dealing with feedstocks with high free fatty acid

content. The procedure is relatively simple and can be carried out in mild weather. Furthermore, the process can convert free fatty acids into esters, increasing the yield of biodiesel production. The acid catalyst used in the reaction is critical in determining the reaction's conversion rate. Because of their high catalytic activity and low cost, sulfuric acid and hydrochloric acid are common catalysts for the esterification reaction. However, the use of such strong acids can result in the formation of undesirable byproducts, which can affect the final product's quality [7], [8].

Recent research has concentrated on the development of alternative esterification catalysts, such as solid acid catalysts and enzymatic catalysts. These catalysts have shown promising results in terms of improving reaction selectivity and yield while reducing the formation of unwanted byproducts. Besides, using alternative catalysts can reduce the environmental impact of the biodiesel production process [9], [10]. Esterification's reaction is presented in Figure 1 below:

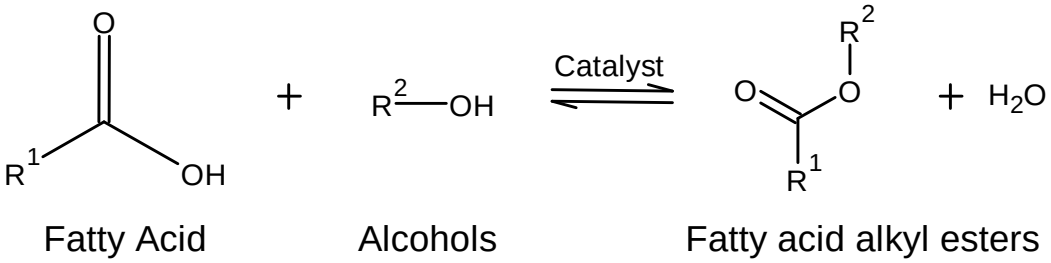

Figure 1. Esterification reaction.
Source: Adapted from [8]

2.2.2 Transesterification

Transesterification is a chemical reaction that has gained widespread acceptance in the production of biodiesel due to its ease of use and low cost. The transesterification reaction produces esters from long-chain fatty acids, which are identified as biodiesel. In this process, a vegetable oil or animal fat reacts with a short-chain alcohol, such as methanol or ethanol, in the presence of a catalyst to produce biodiesel and glycerol. Acids, bases, and enzymes are the most commonly used catalysts in transesterification. While all three types of catalysts proved to be effective at catalyzing the reaction, basic catalysts were found to have a faster reaction rate than acid catalysts due to the formation of a more reactive intermediate [11].

Transesterification is preferred for biodiesel production because it reduces the product's viscosity, making it more suitable for use in conventional diesel engines. Furthermore, the reaction can be performed in mild conditions and on the industrial level, making the biodiesel production process profitable. Despite the many benefits of transesterification, the choice of catalyst is influenced by the specific production conditions and raw material properties [7]. The general chemical reaction from the biodiesel transesterification is shown below in Figure 2.

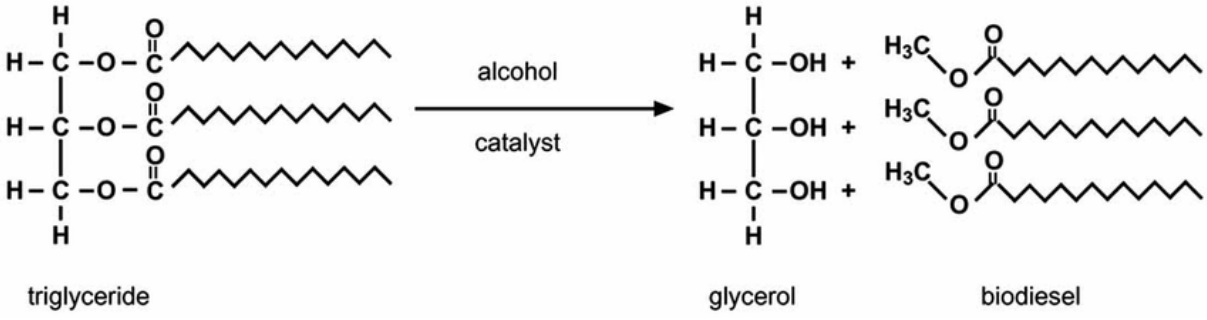

Figure 2. Transesterification reaction.
Source: Adapted from [8]

2.3 Catalysts for biodiesel production

Catalysts are used to speed up the reaction for biodiesel production while also promoting product formation. They are divided into three types: heterogeneous acid and basic catalysts, homogeneous acid and basic catalysts, and enzymatic catalysts. All of these catalysts are attempts to make biodiesel production more economically and environmentally feasible, making the production of this green fuel even more environmentally friendly. This topic will discuss briefly the most commonly used catalysts for each category, as well as the reasons for their selection.

2.4 Heterogeneous catalysts

Using heterogeneous catalysts to synthesize biodiesel has several advantages. Unlike homogeneous catalysis, heterogeneous catalysis allows for easier separation of the catalyst from the final reaction products, as well as the possibility of recovering and reusing the catalyst, which is required in continuous production regimes, and does not promote saponification or corrosion. Heterogeneous catalysis for

transesterification in biodiesel production aims to improve production efficiency and reaction product quality [12].

2.4.1 Heterogeneous basic catalyst

In the transesterification reaction, basic catalysts are more common, such as SrO (strontium oxide) can be used. SrO has a low affinity for methanol and can be reused up to ten times without losing much efficiency. The main disadvantage of SrO is its high cost, with an Apollo Scientific market price of €226 for 100 g, needed to be obtained for somewhere else. CaO (calcium oxide) is an alternative basic catalyst that can be produced relatively easily from calcium hydroxide and calcium nitrate. CaO can be easily obtained from natural sources, such as chicken eggshells and bones, lowering production costs significantly. CaO, on the other hand, necessitates a thermal activation step to remove the adsorbed CO_2 and moisture, and this step should be carried out in an inert atmosphere to avoid carbonation. Choosing an ideal heterogeneous catalyst for biodiesel production necessitates careful consideration of numerous factors such as recovery, reusability, environmental impact, and cost. Although SrO is a highly efficient catalyst, its high cost prevents it from being widely used. CaO, on the other hand, is a promising alternative with low costs and plentiful natural sources. However, its thermal activation step and carbonation susceptibility necessitate extra care during the experimental process [13], [14], [15].

2.4.2 Heterogeneous acid catalyst

Acid catalysts are not as commonly used in transesterification reactions with heterogeneous catalysts, as basic catalysts are known to favor the formation of biodiesel esters more effectively. Acid catalysts are commonly used in the pretreatment of biodiesel, specifically in the esterification reaction to reduce the FFA content., however there are studies that demonstrate that heterogeneous acid catalysts typically have lower esterification activity, but they are advantageous for low quality oil feed stock with a high FFA content [16]. One important aspect of these heterogeneous catalysts is that esterification and transesterification reactions can be conducted simultaneously, eliminating the need for pre-treatment of the oil used [17].

The most common heterogeneous acid catalysts are sulfonated catalysts [16], [18], [19], zeolites [15], [19], [20] and heteropoly acids [19], [20], [21].

Table 2 summarizes commonly used heterogeneous catalysts in biodiesel production. It provides information on prevalent catalysts and relevant biodiesel production process characteristics, such as temperature, and alcohol:oil molar proportion.

Table 2. Revision on heterogeneous catalyst used for biodiesel production.

Catalyst	Feed stock	Alcohol	Alcohol: oil	Temperature	Yield (%)	FAME (%)	Ref
Li/Zn-Cb_2	Waste Canola Oil	MeOH	18:1	60 °C	-	98%	[22]
CaO	Rubber Seed Oil	MeOH	12:1	65 °C	-	99.7%	[23]
CaO	Soybean Oil	MeOH	12:1	-	-	99%	[24]
Fish Bones (CaO)	Waste Cooking Oil	MeOH	10:1	65°C	89.5%	-	[25]
CaO/Al_2O_3	Refined Palm Oil	MeOH	15:1	60°C	86.38%	97.66%	[26]
Calcined Clamshell (CaO)	Waste Frying Oil	MeOH	6.03:1	59.85°C	89.91%	97.74%	[27]
Calcined Eggshells (CaO)	Rubber Seed Oil	MeOH	9:1	65 °C	-	97.84%	[28]
Ostrich Bones (CaO)	Waste Cooking Oil	MeOH	15:1	60 °C	90.5%	-	[29]
Plantain peels/Crab Shell (CaO)	Waste Cooking Oil	MeOH	13.03:1	60 °C	93%	-	[30]
Zn-doped CaO (nanocatalyst)	Calophyllum inophyllum oil	MeOH	9:1	55 °C	89%	-	[31]

As it can be observed, basic heterogeneous catalysts are more commonly used and popular in the academic field, mainly due to the fact that calcium oxide can be obtained from disposable sources such as bones and eggshells, while still achieving satisfactory conversions, thus reducing the cost of biodiesel production and ensuring the production of high-quality biodiesel.

2.5 Homogeneous catalysts

Biodiesel is commonly produced using homogeneous catalysts, which are preferred due to their simplicity and faster reaction time. Homogeneous catalysts are frequently dissolved in the same solvent as all of the reactants, making them easier to use. However, most studies suggest that for efficient biodiesel production with homogeneous catalysts, the free fatty acid (FFA) content should be less than 2% [21].

When compared to heterogeneously catalyzed reactions, homogeneously catalyzed reactions are typically faster and require less catalyst loading. As said previously, the main disadvantage of homogeneous catalysts is that they are difficult and often inefficient to separate from the medium, making reusing the catalysts impossible [32].

2.5.1 Homogeneous basic catalysts

Alkaline catalysts are widely used in the transesterification process for biodiesel production. In commercial transesterification processes, alkaline catalysts are the most commonly used due to their efficiency and cost-effectiveness. It has been reported that the rate of base-catalyzed reactions is reported to be 4,000 times faster than that of acid-catalyzed ones. The most common catalysts are: alkali metal-based hydroxides, namely, sodium or potassium hydroxide; alkali metal-based oxides such as sodium and potassium methoxides; and carbonates [32]. For biodiesel production using a homogeneous catalyst, most studies recommend an FFA content of less than 2 wt.% [21] In summary, alkaline catalysts are highly effective for biodiesel production, and their concentration should be carefully controlled within the optimal range to avoid unnecessary costs. Additionally, proper starting materials are essential for successful transesterification.

When dealing with the production of biodiesel, the presence of free fatty acids (FFA) in the feedstock can pose a challenge. High levels of FFA can result in soap formation during the transesterification process when using basic catalysts, which hinders the production of biodiesel. To overcome this issue, the amount of catalyst used must be carefully controlled. Additionally, to reduce the FFA content, an esterification step can be implemented prior to transesterification. The esterification process converts FFA into esters, which enhances the overall conversion of feedstock into biodiesel. This process reduces the concentration of acids and increases the concentration of esters in the medium, favoring transesterification [33]. Table 3 shows a literature review of some homogeneous basic catalysts.

Table 3. Homogeneous basic catalysis review.

Catalyst	Feedstock	Catalyst (%) / Temp (°C) / A:O	Reaction time (h)	Yield/Conversion (%)	References
KOH	Karanja	1/60/10:1	1.5	92	[34]
KOH	Karanja	1/65/6:1	2	98	[35]
KOH	Pongamia Pinnata	1/60/10:1	1.5	92	[34]
KOH	WPO	1.2/60/6:1	2	95.6	[36]
KOH	Esterified WCO	1/60/3:1	1	94	[37]
KOH	Palm kernel	1/60/6:1	1	96	[38]
KOH	Jatropha	1/50/6:1	2	97.1	[39]
KOH	Jatropha	2.09/60/7.5:1	1	80.5	[40]
KOH	Mahua	0.75/55-56/6:1	1	95.71	[41]
KOH	Mahua	1/45/6:1	3	95	[42]
KOH	Mahua	0.7/60/6:1	0.5	98	[43]
KOH	Mix Karanj and Mahua	0.75/55-56/6:1	1	94	[41]
KOH	Manilkara zapota oil	1/50/6:1	1.5	94.63	[44]
KOH	Camelina sativa oil	1.5/38.7/7.7:1	0.67	97	[45]
KOH	Rapeseed oil	1/65/6:1	2	96	[46]
KOH	Refined cottonseed oil	0.6/55/6:1	1	96	[47]
KOH	Papaya seed oil	1/45/10:1	1	96.46	[48]
KOH	Tobacco seed oil	0.5/50/5:1	1	96.5	[49]
KOH	E.S oleosa oil	1/55/8:1	1.5	96	[50]
NaOH	Palm	1/60/6:1	0.5	95	[51]
NaOH	Neem	0.7/60-75/10:1	6.5-8	88-94	[52]
NaOH	Jatropha	1/60/6:1	1	98	[53]
NaOH	Jatropha	3.3/65/0.7:1	2	55	[54]
NaOH	Jatropha	0.8/45/9:1	0.5	96.3	[55]
NaOH	Sunflower	1/60/6:1	2	97.1	[56]
NaOH	Sunflower	0.6/60/6:1	1	76-97	[36]
NaOH	WCO	1.1/70/7.5:1	0.5	85.3	[57]
NaOH	WCO	0.6/60/4.8:1	0.6	98	[58]
NaOH	Restaurant WCO	0.3 (g)/55/35(v/v)	1.5	85.5	[59]
NaOH	Microalgae	3.5/50/8:1	1.22	87.421	[60]
NaOH	Tobacco seed oil	1/50/5:1	1	97	[49]
NaOH	E.S oleosa oil	1/55/8:1	1.5	93	[50]

Adapted from [61]

2.5.2 Homogeneous acid catalysts

Acid catalysts, in addition to base catalysts, have been extensively investigated for their potential role in biodiesel production. Unlike alkaline catalysts, acid catalysts are less affected by the presence of free fatty acids (FFA) in the oil, as they have the ability to simultaneously catalyze both FFA and triglycerides. However, it is worth noting that the transesterification process using acid catalysts is typically slower, requiring longer reaction times to achieve high biodiesel conversion.

Due to the slower reaction kinetics, homogeneous acid catalysts are not commonly employed in single-step biodiesel production processes. Instead, they are often utilized for pretreatment purposes. Several studies have reported biodiesel yields exceeding 90% in homogeneous acid-catalyzed transesterification reactions. However, achieving such high yields typically necessitates prolonged reaction times, elevated temperatures, larger quantities of alcohol, and increased catalyst loadings [61]. Table 4 presents a review of some research works that used homogeneous acid catalysts for biodiesel production.

Table 4. Homogeneous acid catalysis review.

Catalyst	Feedstock	Reaction	Catalyst (%) /Temp (°C) /A:O	Reaction time (h)	Yield (%)	Ref
HCl	Soybean	Transesterification	10/70/20:1	45	65	[62]
HCl	Rice bran	Transesterification	10/70/20:1	6	>90	[62]
H_2SO_4	WCO	Esterification	5/60/12:1	3	95.376	[63]
H_2SO_4	WCO	Esterification	1/60/14.7:1	1	93.32	[64]
H_2SO_4	WCO	Esterification + Transesterification	4/95/20:1	10	>90	[65]
H_2SO_4	Used soya been oil	Esterification + Transesterification	6.58/65/12:1	10	75.71	[66]
H_2SO_4	Mahua	Transesterification	6 (v/v)/65-70/7.5:1	5	92	[67]
H_2SO_4	Mahua	Esterification	1.24 (v/v)/60/0.32(v/v)	1.26	>98	[68]
H_2SO_4	Brown grease	Esterification	1.3 mL/65/35 mL	2	99.4	[69]

Table 4. Homogeneous acid catalysis review (continuation).

Catalyst	Feedstock	Reaction	Catalyst (%) /Temp (°C) /A:O	Reaction time (h)	Yield (%)	Ref
H_2SO_4	Microalgae	Transesterification	100/30/56:1	4	60	[70]
H_2SO_4	Karanja oil	Esterification	1.5 mL/54.5-55.5/6:1	1	87.2	[41]
H_2SO_4	Rubber seed oil	Esterification	1.38/50/16:1	2	99.3	[71]
H_2SO_4	Rubber seed oil	Esterification	10.74/65/10:1	1	98.6	[71]
H_2SO_4	Rubber seed	Esterification	0.5/40-50/6:1	0.5	>98	[72]
H_2SO_4	Tobacco	Esterification	1/60/18:1	0.4	91	[73]
H_2SO_4	Soybean	Transesterification	1/65/30:1	69	>90	[74]
H_2SO_4	Microalgae	Transesterification	3.361/50/8:1	1	89.58	[60]
H_2SO_4	Castor oil	Transesterification	0.2 molar ratio/80/6:1	8	80	[75]
H_2SO_4	Castor oil	Esterification	1/50/20:1	1	90.83	[76]
H_2SO_4	Castor oil	Esterification	1/50/15:1	2.09	73.27	[77]

Overall, while acid catalysts offer certain advantages in terms of their ability to handle FFA, their slower reaction kinetics and the need for more rigorous reaction conditions make them less commonly used in comparison to alkaline catalysts. Nonetheless, further research is being conducted to explore ways to optimize the efficiency and feasibility of acid-catalyzed biodiesel production processes.

2.6 Biocatalysts

A search for biocatalysts in the production of biodiesel has become increasingly popular due to the need for more sustainable and efficient methods of energy generation. Biocatalysts offer numerous advantages, including high selectivity, low toxicity, and the ability to operate under milder conditions. By reducing reliance on traditional chemical catalysts, the use of biocatalysts can significantly lower the environmental impact of biodiesel production, promoting sustainability in the process. As such, the search for new and improved biocatalysts continues to be a key focus in the field of sustainable energy research.

One of the most used biocatalysts for the biodiesel production is lipases. Lipases, also referred to as triacylglycerol acyl hydrolases, are enzymes with

remarkable lipolytic properties that have gained prominence as substitutes for chemical catalysts in modern organic chemistry. Their appeal lies in their wide range of chemobiological activities, as well as their ability to exhibit substrate specificity, functional group specificity, and enantioselectivity. Lipases have proven to be valuable in various organic reactions, including acidolysis, hydrolysis, epoxidation, esterification, alcoholysis, amination, and transesterification, among others [78].

Lipases present distinct advantages over traditional chemical catalysts in the production of biodiesel. One notable advantage is their ability to operate efficiently at ambient temperatures, eliminating the need for high temperature conditions required by chemical catalysts, as seen in the tables above, most of the reactions were carried in a temperature that does not meet with a room temperature. So, the lipases are interesting cause this not only reduces energy consumption but also lowers production costs associated with heating. Furthermore, lipases exhibit remarkable tolerance towards various feedstocks, enabling their utilization with diverse raw materials, thus enhancing the flexibility and sustainability of biodiesel production processes [21], [78].

Lipases can be employed in two distinct forms: immobilized and free. In the context of biodiesel production, the utilization of immobilized lipase has gained considerable attention owing to its manifold advantages. As a heterogeneous catalyst, immobilized lipase offers the unique advantage of being recoverable and reusable, in contrast to free lipase which is challenging to recover. The substantial cost associated with lipases further underscores the significance of recovery and reuse as pivotal considerations. The most evident disadvantage of these types of catalysts is the reaction rate, which tends to be lower compared to chemical catalysts. Moreover, immobilized lipase exhibits enhanced thermal stability, rendering it more amenable to practical applications, especially at elevated temperatures. In the research study documented in [14] it was concluded that free lipase does not offer any discernible advantages over immobilized lipase in the specific context of biodiesel production. Notably, immobilized lipases not only demonstrate superior biodiesel conversion efficiency but also exhibit wider operational flexibility encompassing pH and temperature ranges. Table 5 displays the advantages and disadvantages of using immobilized lipases and free lipases.

Table 5. Comparison between use of different types of lipases as catalysts.

	Free Lipase Catalyst [79], [80], [81], [82], [83]	Immobilized Lipase Catalyst [84], [85], [86], [87]
Reaction Rate	Low	Low
Catalyst Recovery	Difficult	Easy
Catalyst Reuse	Difficult	Easy
Cost	High	Moderate
Purification of biodiesel	Easy	Easy
Biodiesel Yield	High	High

Adapted from [14]

2.6.1 Green immobilized lipases

The issue of enzyme recovery in free lipase systems can be effectively addressed by immobilizing the enzyme onto a solid support. When in their "solid" state, lipases exhibit low contamination in the reaction medium, resembling traditional heterogeneous catalysts. They also demonstrate increased resistance to external factors compared to their unsupported counterparts. There are several techniques available for lipase immobilization, with the most popular ones being encapsulation, adsorption, covalent binding, and cross-linked enzyme aggregates and crystals. However, these techniques often employ petroleum-derived immobilizing agents, which can contribute to environmental concerns when the catalyst is disposed of after use. Thus, simply substituting chemical catalysts with biological ones does not fully address the issue if the immobilizing agents themselves are derived from petroleum sources. In this regard, organic immobilizing agents can be employed as alternatives, as they do not pose the same environmental disposal concerns [78], [88].

Therefore, the use of solid supports for lipase immobilization provides a practical solution to enhance enzyme recovery and minimize environmental impact. By employing organic immobilizing agents instead of petroleum-derived ones, the overall sustainability of the immobilization process can be improved, making it more compatible with the principles of green chemistry and biocatalysis. Table 6 presents

some techniques used and the corresponding supports employed in the production of bioimmobilized lipases.

Table 6. Green immobilized catalyst review.

Lipase	Technique	Sustanability metric	Product Yield	Cycles	Ref
T. lanuginosus	Rice straw modified with Fe_2O_3 nanoparticles for lipase crosslinking with glutaraldehyde.	Use of rice straw as lipase carriers	83% FAME	10	[89]
Aspergillus niger	Submerged fermentation of myceliumbound lipase in cornmeal, molasses, waste cooking oil, milk serum, etc.	Fungi cells cultivated in agroindustrial waste	96% FABE	Several	[90]
Aspergillus oryzae	Magnetic cross-linked enzyme aggregates (mCLEAs) co-fed with bovine serum albumin.	Replaced glutaraldehyde with bovine serum albumin	95% FAME	5	[91]
Candida antarctica	Tannic acid-magnetic cross-linked enzyme aggregates with starch as crosslinker.	Using starch as crosslinker	85.9% FAPE	7	[92]
Porcine pancreas lipase	Genipin for cross-linking chitosan beads towards immobilization.	Use of genipin, a fruit extract, as a glutaraldehyde substitute	92.3% FAME	10	[93]
T. lanuginosus	Adsorption immobilization in polyurethane foams obtained from bio polyol enzymatic glycerolysis of castor oil and glycerol.	Use of glycerol, a biodiesel byproduct and castor oil for polyurethane synthesis	66% FAME	6	[94]
Candida antarctica	CLEA preparation onto octyl-modified mesocellular foams with oxidized sodium alginate.	Oxidized sodium alginate was used to substitute	89.0% FAME	5	[95]

2.7 Nanocatalyst

Nanocatalysts have recently been studied for their high selectivity, activity, efficiency, and potential for reuse, thereby reducing operation costs. The use of nanocatalysts is gaining attention due to the challenges associated with heterogeneous catalysts, which rely on their surface area and particle shape to drive reactions with high yields. Nanocatalysts overcome these issues by possessing a high surface area and significant porosity. Additionally, nanocatalysts enable reactions to occur at non-extreme temperatures with relatively short reaction times, depending on the intended purpose of the study [96], [97].

Nowadays, two types of nanocatalyst are being studied: magnetic and nonmagnetic.

2.7.1 Magnetic nanocatalysts

At present, attractive nanocatalysts are preferred over mass catalysts. This is due to the lack of mass exchange resistance and rapid deactivation, as well as the high recovery rate within the department. Attractive functionalized magnetic nanocatalysts are getting more attention for biodiesel production. Its high recovery is attributed to its magnetic separation capability, eliminating the need for equipment-intensive techniques or filtration, thus simplifying the recovery process. This also contributes to its environmentally friendly nature, as the disposal can be easily and properly carried out [97]. Most magnetic nanocatalysts are mixed with iron oxides, with the variation lying in the additional components that are mixed in. The most common among them is calcium oxide, which can be obtained from various sources, as mentioned in the topic of heterogeneous basic catalysts above.

Table 7 shows some magnetic nanocatalysts there are used in biodiesel production.

Table 7. Magnetic nanocatalyst review

Feedstock	Catalyst	Catalyst (%)	Temperature (°C)	M:O	Time (h)	Biodiesel Yield (%)	Ref
Chicken Fat	CaO/CuFe	3	70	15:1	4	94.52	[98]
Jatropha oil	$CaSO_4/Fe_2O_3$-SiO_2	12	120	9:1	4	94	[99]
Rapeseed oil	K-Fe_3O_4-CeO_2	4.5	65	7:1	2	96.13	[100]
Soybean oil	CaO@γ-Fe_2O_3	2	70	15:1	3	98.8	[101]
Chicken Fat	AC/$CuFe_2O_3$@CaO	3	65	12:1	2	95.6	[102]
Soybean oil	Fe_3O_4/MCM 41/ECH/Na_2SiO_3	3	-	25:1	8	99.2	[103]
Soybean oil	$MgFe_2O_4$@CaO	1	70	12:1	3	98.3	[104]
Soybean oil	CaO/$CoFe_2O_4$	1	70	15:1	5	87.4	[105]
Sunflower oil	$CsH_2PW_{12}O_{40}$/Fe-SiO_2	4	60	12:1	4	81	[106]
Sunflower oil	Cs/Al/ Fe_3O_4	6	58	14:1	2	94.8	[107]
Seed oil	CaO- Fe_3O_4	10	65	20:1	5	69.7	[108]
Canola oil	ZnO/$BiFeO_3$	4	65	15:1	5	95.43	[109]
Soybean oil	Fe_3O_4@Gly	1.5	65	15:1	3	95.8	[110]
Sunflower oil	MgO/$MgFe_2O_4$	4	110	12:1	4	91.2	[111]

Adapted from [112]

2.7.2 Nonmagnetic nanocatalysts

The main difference between non-magnetic and magnetic catalysts lies in their recovery process. Magnetic catalysts offer the advantage of lower total production costs due to their efficient recovery. However, non-magnetic catalysts can also be used in production. The most commonly used non-magnetic nanocatalysts in biodiesel production include metal oxides, sulfated oxides, hydrotalcite, zeolites, and zirconia.

Examples of catalysts can be seen in Table 8.

Table 8. Nonmagnetic nanocatalyst review.

Feedstock	Catalyst	Catalyst (%)	Temperature (°C)	M:O	Time (h)	Biodiesel Yield (%)	Ref
Mesua ferrea oil	Co/ZnO	2.5	60	9:1	3	98.03	[113]
Palm oil	$NaAlO_2$/γ-Al_2O_3	10.89	64.72	20.79:1	3	97.65	[114]
Castor oil	Ni-doped ZnO	11.07	55	8:1	1	95.20	[115]
Waste oil	Na_2O impregnated-CNTs	5	90	20:1	4	97.6	[116]
Soybean oil	ZrO_2 loaded with $KC_4H_5O_6$	6	60	16:1	2	98.03	[117]
Chinese tallow seed oil	KF/CaO	4	65	12:1	2.5	96.8	[118]
Soybean oil	KNa/ZIF-8	-	100	10:1	3.5	98	[119]

Adapted from [97]

2.8 Advantages of each catalyst

Considering each author's purpose and objective in conducting reactions for biodiesel production, whether using transesterification or esterification processes, an economic and chemical analysis should be performed to optimize the goals of each study. Therefore, Table 9 illustrates the advantages and disadvantages of each catalyst presented in the aforementioned topics.

Table 9. Comparison between different types of catalysts.

Type of catalyst	Advantages	Disadvantages
Heterogeneous Basic Catalyst	Easy separation, catalyst reuse, good selectivity, low activation energy, and low-cost sources (CaO)	The catalyst can be poisoned when exposed to atmospheric air during preparation (CaO)
Heterogeneous Acid Catalyst	Prevents saponification, promotes FFA formation, ease of catalyst reproduction and regeneration, transesterification and esterification occur	Slow reaction, high activation energy
Homogeneous Basic Catalyst	Low cost, high conversion, low activation energy, easy accessibility	Not environmentally friendly, cannot be reused, requires several washes
Homogeneous Acid Catalyst	High yield in biodiesel production, prevents saponification	Low reaction rate, cannot be reused, corrosive, high activation energy
Biocatalyst	High selectivity, low toxicity, low activation energy, high yield in biodiesel production	Moderate/high cost, low reaction rate, depends on the type of alcohol
Nanocatalyst	High surface area, facilitated separation (magnetic), low toxicity, environmentally friendly, low activation energy, fast reaction	High cost in its preparation

2.9 Biodiesel Purification

Several requirements must be fulfilled for biodiesel must be followed for biodiesel to be used in vehicle engines, as after biodiesel production, it contains impurities such as glycerol, residual alcohol, and solid impurities depending on the oil used for its production. These requirements may vary depending on the location, with

EN 14214 being the standard followed in Europe and ASTM D6751 being followed in the United States [120].

Table 10 provides a comparison of the properties requirements that must be followed according to each standard

Table 10. Comparison between European and American standards requirements.

Properties	**EN 14214**	**ASTM D6751**
Composition of Biodiesel	C12-C22	C12-C22
Esters Content [wt/wt]	≥ 96.5%	-
Density at 15 °C [kg/m³]	860-900	-
Viscosity at 40 °C [mm²/s]	3.50-5.00	1.9-6
Flash Point [°C]	≥ 101	≥ 130
Sulphur Content [mg/kg]	≤ 10	≤ 50
Carbon Residue [wt/wt]	≤ 0.3%	≤ 0.05%
Cetane Number	≥ 51	≥ 47
Sulfated Ash [wt/wt]	≤ 0.02%	≤ 0.02%
Water Content	≤ 500 mg/kg	≤ 0.05 % (v/v)
Corrosion	Class 1	3h
Oxidative Stability 110°C	≥ 8h	≥ 3h
Acid Value [mg KOH/g]	≤ 0.50	≤ 0.50
Methanol [wt/wt]	≥ 0.2%	-
Monoacylglycerols [wt/wt]	≤ 0.7	-
Diacylglycerols [wt/wt]	≤ 0.2%	-
Tryacylglycerols [wt/wt]	≤ 0.2%	-
Free Glycerin [wt/wt]	≤ 0.02%	≤ 0.2%
Total Glycerin [wt/wt]	≤ 0.25%	≤ 0.25%
Pour Point [°C]	-	-15 to -16
Phosphorus Amount	≤ 4 mg/kg	≤ 0.001% (w/w)
Cloud Point [°C]	-	-3 to -12 °C

Adapted from [121]

3. ADSORPTION

Adsorption is a process where molecules, atoms, or ions (adsorbate) adhere to the surface of a solid or liquid (adsorbent) due to physical or chemical interactions. The adsorbate is the substance that accumulates on the adsorbent's surface. This process is crucial in various applications, such as water and air purification, where materials like activated carbon and silica gel act as effective adsorbents. The efficiency of adsorption depends on the properties of both the adsorbate and the adsorbent, including surface area, pore size, and chemical compatibility. Adsorption can be classified into physical adsorption, which involves weak van der Waals forces, and chemical adsorption, which involves stronger chemical bonds [122].

Adsorption is widely employed in various industries, particularly for water treatment, removal of pollutants from a specific compound, catalytic processes, and more. The adsorption process can be applied to avoid washing in the biodiesel production process for glycerol removal. In this context, inexpensive materials can be used for adsorption, which would otherwise be discarded in nature. For instance, in this study, nut shells will be utilized for the purification of biodiesel using adsorption process [123].

3.1 Adsorbents for biodiesel purification

To avoid wet washing, adsorption can be used as an alternative to address the high-water consumption in biodiesel purification. Up to 3 liters of water can be used per liter of biodiesel produced [120]. In 2022, Brazil produced 6.7 billion liters of fuel [124], resulting in the usage of 20.1 billion liters of water for production, which represents a significant amount. Therefore, the utilization of adsorbents in biodiesel purification is an interesting approach to avoid water waste. These adsorbents can be derived from inexpensive and disposable raw materials such as banana peels, sugarcane bagasse, rice husks, mushroom powder, chamotte clay, and others [125]. In their study, [126] employed various natural adsorbents and a commercial adsorbent called "Select 450®". A comparison was made between the different adsorbents, and it was demonstrated that some of the natural adsorbents performed better than the commercial adsorbent, as shown in the table below.

Table 11. Some research results of adsorption for biodiesel purification.

Adsorbent	Acidity Index (mg KOH/g)	Adsorbent Amount (w/v)	Free Glycerine (%)
Biodiesel Sample	**0.172 ± 0.027**		**0.129 ± 0.001**
Potato starch	0.111 ± 0.003	1%	0.006 ± 0.003
Potato starch	0.114 ± 0.001	2%	0.006 ± 0.003
Potato starch	0.106 ± 0.004	5%	0.000 ± 0.001
Potato starch	0.100 ± 0.009	10%	0.023 ± 0.001
Corn starch	0.120 ± 0.008	1%	0.052 ± 0.001
Corn starch	0.106 ± 0.008	2%	0.007 ± 0.002
Corn starch	0.129 ± 0.001	5%	0.030 ± 0.001
Corn starch	0.104 ± 0.008	10%	0.006 ± 0.003
Cassava starch	0.099 ± 0.001	1%	0.000 ± 0.001
Cassava starch	0.099 ± 0.001	5%	0.007 ± 0.002
Cassava starch	0.099 ± 0.001	10%	0.022 ± 0.001
Rice starch	0.100 ± 0.001	1%	0.000 ± 0.001
Rice starch	0.097 ± 0.002	2%	0.007 ± 0.002
Rice starch	0.100 ± 0.001	5%	0.000 ± 0.001
Rice starch	0.098 ± 0.002	10%	0.007 ± 0.002
Celulose	0.097 ± 0.002	1%	0.029 ± 0.001
Celulose	0.099 ± 0.001	2%	0.015 ± 0.001
Celulose	0.099 ± 0.001	5%	0.068 ± 0.001
Celulose	0.099 ± 0.001	10%	0.000 ± 0.001
Select 450@	0.198 ± 0.001	1%	-
Select 450@	0.101 ± 0.001	2%	0.008 ± 0.002
Select 450@	0.093 ± 0.005	5%	0.047 ± 0.001
Select 450@	0.099 ± 0.002	10%	0.008 ± 0.002
Limit EN 14214	**0.5**		**0.02**

Adapted from [126]

3.2 Activated carbons

The use of adsorption using activated carbons obtained from different biomass wastes can be an alternative adsorbent for biodiesel purification and can be derived from organic waste materials. In the production of activated carbon, a high concentration of lignin is desirable due to its high carbon content. Some examples of organic waste materials used as raw materials for activated carbon include walnut shells, chestnut shells, rice husks, hazelnut shells, sugarcane bagasse, peanut shells,

among others [127], [128], [129], [130], [131], [132]. Activated carbons possess a large internal surface area and a highly porous structure, which results in their high adsorption capacity. They also have functional groups on their surface, and the properties of each activated carbon can vary depending on the method of activation, whether it is chemical or physical. These functional groups can interact with substances in the solution, potentially altering the pH and influencing the adsorption process [133].

Chemical activation involves the use of impregnating agents, such as alkaline substances like sodium hydroxide (NaOH), potassium hydroxide (KOH), calcium chloride ($CaCl_2$), and acidic compounds like phosphoric acid (H_3PO_4) and sulfuric acid (H_2SO_4). Metal salts like zinc chloride ($ZnCl_2$) can also be used. One advantage of chemical activation is that it requires lower temperatures during the preparation process compared to physical activation, making it more energy-efficient. Additionally, the impregnating agents used in chemical activation are relatively cost-effective. On the other hand, physical activation does not rely on chemical impregnating agents to create pores. Instead, it involves higher operating temperatures, typically ranging from 800 to 1100°C. In contrast, chemical activation can be conducted at lower temperatures, usually between 400 and 900°C [134].

3.3 Adsorption isotherms

Adsorption isotherms can help with the information about the adsorbent, this method enables us to draw conclusions regarding the favorability of the adsorption process in a given experiment. By analyzing the obtained curves and comparing them to known benchmarks, we can assess whether the adsorption is favorable or unfavorable under the specific experimental conditions. This information is crucial for evaluating the effectiveness of the adsorbent and optimizing the adsorption process for various applications. By knowing the initial adsorbate concentration (C_0), the volume of solution used (V), the mass of the adsorbent employed (m), and the equilibrium adsorbate concentration (C_e), equation 1 can be derived. This equation allows for the determination of important parameters in adsorption studies, facilitating the characterization and optimization of adsorption processes. In this article, we will

explore the significance of this equation and its implications for understanding adsorption phenomena.

$$q = \frac{V}{m}(C_0 - C_e) \qquad (1)$$

By plotting the quantity adsorbed (q) on the y-axis against the equilibrium concentration (C_e) on the x-axis, an adsorption isotherm can be constructed. As the name suggests, its experimental measurement should be conducted at a constant temperature, as temperature can affect the adsorption kinetic constant, thereby influencing the overall process.

Figure 3 presents some of the typical equilibrium adsorption isotherm shapes and in Table 12 are presented four of the most commonly used mathematical models used to describe the experimental adsorption behaviour.

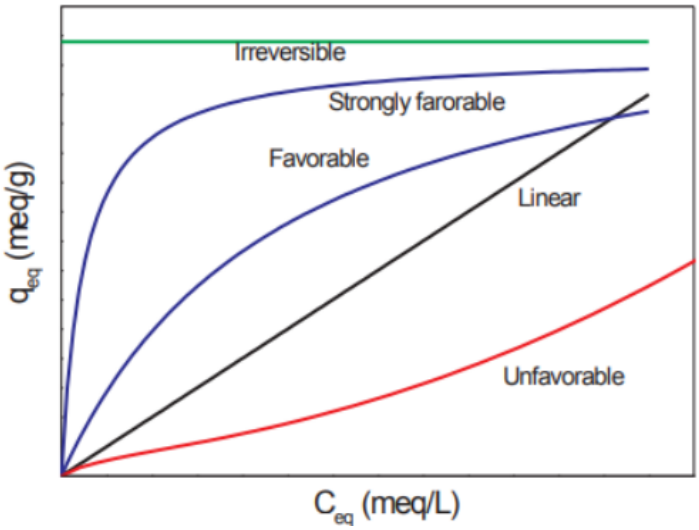

Figure 3. Most common isotherms shapes.
Source: [135]

Table 12. Isotherms models

Model	Equation	Parameters
Freundlich	$q_e = K_f C_e^{\,1/n_f}$	$K_f\ (mg\ g^{-1})(mg\ g^{-1})^{-1/n_f}$ n_f
Sips	$q_e = \frac{q_s K_s C_e^{n_s}}{1 + K_s C_e^{n_s}}$	$q_s\ (mg\ g^{-1})$ $K_s\ (g\ mg^{-1})^{n_s}$ n_s
Liu	$q_e = \frac{q_{liu} C_e^{n_{liu}}}{K_{liu}^{n_{liu}} + C_e^{n_{liu}}}$	$q_{liu}\ (mg\ g^{-1})$ $K_{liu}\ (mg\ g^{-1})$ n_{liu}

Table 12. Isotherms models (continuation).

Model	Equation	Parameters
Radke-Prausnitz	$q_e = \frac{abC_e^m}{a + bC_e^{m-1}}$	$a\ (g\ /g)$ $b\ [(mg\ g^{-1})/(mg\ g^{-1})^m]$ m

The Freundlich adsorption isotherm model describes a reversible and non-ideal adsorption process, suitable for multilayer adsorption on heterogeneous surfaces.

Initially developed for animal charcoal adsorption, the Freundlich model is widely applied in the adsorption of organic compounds and systems with molecular sieves or activated carbon. The model's expression highlights the exponential distribution of active sites and their energies, with the stronger binding sites being occupied first. This model is applicable to heterogeneous surfaces. The value of 1/n indicates surface heterogeneity and adsorption favorability: 0 < 1/n < 1 indicates favorable adsorption, 1/n > 1 is unfavorable, and 1/n = 1 is irreversible [136].

The Sips isotherm model combines the Freundlich and Langmuir models to predict the heterogeneity of adsorption systems and overcome the limitations of high concentrations in the Freundlich model. This results in an expression with a finite limit at high concentrations, adsorption without adsorbate-adsorbate interaction [136].

To describe the biosorption of metal ions by microbial aggregates, Yu Liu and colleagues proposed a biosorption model using a thermodynamic approach. The model considers the adsorbed phase concentration (q_e), biosorption capacity (q_{liu}), fluid phase concentration (C_e) and the equilibrium constant (K_{liu}) [137].

Liu presented the equation in their article being:

$$q_e = \frac{q_{liu} C_e^{n_{liu}}}{K_{liu}^{n_{liu}} + C_e^{n_{liu}}} \quad (2)$$

The Radke-Prausnitz isotherm model is typically applied in adsorption systems when the adsorbate concentration is relatively low. This model has been used to elucidate the adsorption characteristics of micropollutants such as p-cresol and p-chlorophenol onto activated carbon [138].

In summary, each adsorption isotherm model has specific characteristics that make it suitable for different types of systems and adsorption conditions, ranging from heterogeneous surfaces to specific adsorbate concentrations.

The Table 12 presents the equations of the isotherms models that were selected to study the experimental adsorption behavior of glycerol on the prepared biomass adsorbents.

3.4 Adsorption kinetics

Adsorption kinetic models are used to evaluate adsorbent performance and investigate the mechanisms of mass transfer during adsorption. These models provide valuable information about the adsorption capacity of the adsorbent. Specifically, "qe" represents the maximum amount of adsorbate that the adsorbent can retain at equilibrium, while "qt" denotes the amount of adsorbate adsorbed per unit mass of the adsorbent at any given time "t". The equilibrium time indicates the point at which the adsorbent becomes saturated and can no longer adsorb additional molecules.

Some mathematical models, such as pseudo-first order (PFO), pseudo-second order (PSO) and intraparticle diffusion (IPD), used for fitting experimental data are shown in the Table 13 below.

Table 13. Adsorption kinetics models.

Model	Equation	Parameters
PFO model	$q_t = q_e(1 - e^{-k_1 t})$	k_1 – adsorption rate constant (min^{-1}) t - time (min)
PSO model	$q_t = q_e - \frac{q_e}{q_e k_2 t + 1}$	k_2 – adsorption rate constant ($\frac{g}{mg.min}$) t - time (min)
IPD Model	$q_t = k_d t^{\frac{1}{2}} + C$	k_d- Intraparticle diffusion coefficient ($\frac{mg}{g.min^{0.5}}$) C – Diffusion resistance ($\frac{mg}{g}$)
Elovich model	$qt = \frac{1}{\beta}\ln(1 + \alpha\beta t)$	α - initial adsorption rate ($\frac{mg}{g.min}$) β - desorption constant ($\frac{mg}{g}$) t - time (min)

Source: [123], [139]

Lagergren (1898) was the first to propose the pseudo-first order (PFO) model. The pseudo-second order (PSO) model was first used to simulate lead adsorption on peat by [140]. The PSO model was then widely used to describe adsorption processes. The PSO model was used in the majority of published papers to predict adsorption experimental data and calculate adsorption rate constants. The intraparticle diffusion (IPD) model was introduced by Weber and Morris in 1963 to analyze the kinetic data from the adsorption of some organic compounds on the carbon particles [139]. The Elovich model was presented in 1962 by Elovich and Larinov. Elovich's model was made to represent adsorption from systems gas-solid but in the last decades the model is being used also for liquid-solid adsorption [123].

The activation energy involved in the adsorption process can be determined using the Arrhenius linearized equation (Equation 3), based on the adsorption rate constants obtained from the pseudo-first and pseudo-second order equations.

$$\ln k = -\frac{E_a}{RT} + \ln A \qquad (3)$$

k – Kinetic constant (min^{-1});

E_a – Activation energy ($\frac{J}{mol}$);

R – Universal gas constant ($\frac{J}{molK}$);

T – Temperature (K);

A – Collision Frequency (min^{-1}).

4 EXPERIMENTAL METHODOLOGY

4.1 BIODIESEL PRODUCTION

Biodiesel production was carried out using sodium hydroxide (98% purity) from Honeywell as the catalyst, along with absolute ethanol from Carlos Erba.

The raw material used was waste cooking oil from the canteen of the Polytechnic Institute of Bragança. The transesterification reactions took place in a round-bottom flask attached to a reflux condenser at 30°C, with a 1:7.5 oil/alcohol molar ratio and 0.5% catalyst load. The feedstock oil was heated to the reaction temperature, then the ethoxide solution was prepared with sodium hydroxide (0.5% wt/wt) and added to the oil. The mixture was stirred for an hour. Following transesterification, the mixture underwent a 60-minute ethanol recovery using a rotary evaporator (BUCHI – Model R-114) under vacuum (0.150 atm) and a warm bath (60°C).

After the recovery of ethanol, it was left for 24 hours to allow phase separation between the biodiesel and the glycerol-containing phase.

Figure 4. Biodiesel post phase separation.

4.2 BIODIESEL AND OIL CARACTERIZATION

Initially, in this study, characterization of the oil was conducted to assess whether the raw material to be used would require treatment due to its “dirty” nature, and also to gain an understanding of what would be employed for adsorption experiments. Following the oil analysis and biodiesel production, analyses such as glycerol quantification in the produced biodiesel and the percentage of conversion of the raw material into Fatty Acid Ethyl Esters (FAEEs) were performed.

4.2.1 Determination of Acidity Value

The acidity value was employed to quantify the amount of free fatty acids present in the sample of used cooking oil. It was also utilized to determine whether the sample would require esterification treatment before biodiesel production on a larger scale. The acid value of the oil was evaluated according to the European Standard EN 14140:2003. 1g of the sample was weighed and added to 25 mL of a solvent consisting of a 1:1 (v/v) mixture of diethyl ether and anhydrous ethanol from Carlos Erba. Five drops of phenolphthalein were added, followed by titration with a methanolic solution of KOH. The acid value of the oil was calculated using equation 4.

$$IA\left(\frac{mg\ KOH}{g}\right) = \frac{V_{KOH}\ .\ C_{KOH}\ .\ MM_{KOH}}{m_{sample}} \tag{4}$$

IA – Acidity value ($mg\ KOH/g$);
V_{KOH} – Volume of titrant solution (mL);
C_{KOH} – Concentration of standard solution (mol/L);
MM_{KOH} – Molar mass of KOH (g/mol);
$\mathrm{m_{sample}}$ – Mass of sample (g).

4.2.2 Determination of FAEEs

For this analysis, biodiesel samples were prepared in duplicate using catalyst concentrations of 0.5%, 0.6%, and 0.7% (wt/wt) to determine the optimal percentage for the conversion of the oil in fatty acid ethyl esters (FAEEs) for scaled-up biodiesel production. These samples were subsequently analyzed via gas chromatography to assess the percentage of FAEEs produced.

A GC-FID (Gas Chromatography with Flame Ionization Detector) system with an OPTIMA® Biodiesel F column was utilized for these tests, in accordance with EN14103:2003 methodology. This study's methodology used the internal standard method, which included a specific amount of an ester that was not present in the created biodiesel. The peak was then used to compare and determine the amounts of esters in the sample. The internal standard chosen was methyl heptadecanoate (98% purity), from TCI brand.

For the GC-FID analysis, approximately 250 mg of biodiesel was weighed, followed by the addition of 5 mL of the internal standard solution at a concentration of 0.02 M. To ensure the absence of moisture in the sample, anhydrous sodium sulfate was added and allowed to settle. For analysis, 1 mL of the solution was withdrawn and injected into the GC-FID for analysis.

The operational conditions for GC-FID analyses were a 1 mL/min helium flow, an initial temperature of 50 °C for 1 minute, and a ramp of 25 °C/min to a temperature of 200 °C. A second ramp of 3 °C/min was then applied until the temperature reached 230 °C. Each biodiesel sample had a total analysis time of 20 minutes. The injector temperature was kept at 250 °C using a split ratio of 1:25, and the detector was set to the same temperature.

The equipment conditions for the analysis were as follows: a helium flow rate of 1 mL/min, with an initial temperature set at 50°C for one minute, followed by a ramp of 25°C/min until reaching 200°C. A secondary ramp of 3°C/min was then applied to ensure temperature control until reaching 230°C. Each analysis was allowed to run for 20 minutes. The injector temperature was maintained at 250°C, and the detector was held at the same temperature.

4.2.3 Derivatization of Fatty Acids using BF_3

The derivatization of fatty acid esters using boron trifluoride dehydrated (96%) from Sigma-Aldrich was employed to assess the distribution of fatty acids present in raw materials for biodiesel production. Initially, derivatization was conducted, involving the conversion of triglycerides and fatty acids in the sample into methyl esters or ethyl esters, followed by the identification of these compounds through gas chromatography.

In a 20 mL flask, 50 mg of the sample and 2.5 mL of a 0.5 M ethanolic solution of KOH were weighed. The mixture was then placed in an oven at 90°C for 10 minutes, cooled to room temperature, and subsequently, a 1:10 (v/v) ethanolic solution of BF_3 was added to the sample (2 mL) and placed in the oven again at 90°C for 30 minutes. Afterward, it was removed and allowed to cool to room temperature.

Following these steps, 3 mL of internal standard (methyl heptadecanoate) solution with a concentration 0.02 M was added to the sample and thoroughly mixed for homogenization. Subsequently, 2 mL of a sodium chloride solution was added and mixed again. After all these steps, the sample was centrifuged for 5 minutes at 3000 rpm to ensure complete phase separation. Then, 2 mL of the upper phase was extracted for analysis using GC-FID, enabling the determination of the molecular weight of the oil used to proceed with biodiesel production according to equation 5 [141].

$$MM = 3 * \frac{\sum f_i}{\sum \left(\frac{f_i}{MM_i}\right)} + 38.049 \quad (5)$$

Where:

MM – Molar mass (g/mol);

f_i – Mass fraction of fatty acids;

MM_i – Molar mass of each fatty acid (g/mol)

4.2.4 Determination of reaction Yield

The conversion of the raw material into biodiesel can be calculated using equation 6.

$$C(\%) = \frac{m_{light\ phase} \cdot \%FAEE}{m_{raw\ material}} \quad (6)$$

Where:

C – Yield (%);

$m_{light\ phase}$ – Mass of light phase (g);

$\%FAEE$ – Percentage of FAEE (%);

$m_{raw\ material}$ – Mass of the raw material (g).

4.2.5 Glycerol quantification on raw material

For the quantification of glycerol, the use of a gas chromatography column operating at 350°C is recommended [138-140]. However, in this work, an alternative methodology was adopted, which employs indirect quantification using UV-VIS and sodium periodate. This reacts with glycerol to form a yellowish complex.

The methodology utilized [142] involves the oxidation of glycerol in the presence of sodium periodate, leading to the formation of formaldehyde, followed by the reaction with acetylacetone in the presence of ammonium acetate. This results in the formation of the molecule 3,5-diacetyl-1,4-dihydrolutidine, which imparts a yellowish coloration. Consequently, the quantity of glycerol in the sample can be analyzed using UV-VIS spectroscopy at a wavelength of 412 nm. The molecular structure is depicted in Figure 5.

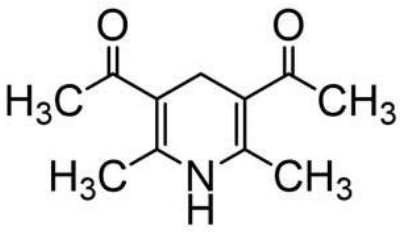

Figure 5. Chemical structure of 3,5-diacetyl-1,4-dihydrolutidine.

For the reaction, the following reagents were used: Sodium periodate from Honeywell, ammonium acetate 98% from Sigma-Aldrich, acetic acid 99.8% from Honeywell, n-Hexane 99% HPLC-isocratic from Carlo Erba, acetylacetone 99% from Sigma-Aldrich, and ethanol 96% from Carlo Erba.

Five solutions were prepared for the reactions, with the first being a 1:1 (v/v) solution of 96% ethanol and ultrapure water. Ultrapure water was chosen to minimize interference in the analysis results. This solution was used as a solvent in the glycerol oxidation reaction and also for glycerol extraction from biodiesel. For the extraction, 4 mL of this solution and 4 mL of n-Hexane were used per 0.2 g – 1 g of biodiesel analyzed. Subsequently, centrifugation was performed at 2100 rpm for 15 minutes to achieve complete phase separation. The denser phase (ethanol) settled at the bottom, containing the extracted glycerol, while the upper phase contained impurities extracted by hexane.

Additionally, solutions prepared with ultrapure water included 1.6 M acetic acid and 4 M ammonium acetate solutions for the reactions. According to [142], these solutions are stable for weeks, so they were stored during the analyses. However, the solutions of 0.2 M acetylacetone and 10 mM sodium periodate needed to be prepared daily. The acetylacetone solution was prepared by mixing 200 µL with 5 mL of 1.6 M acetic acid solution and 5 mL of 4 M ammonium acetate. Meanwhile, the sodium periodate solution was prepared by dissolving 21 mg in 5 mL of 1.6 M acetic acid solution and 5 mL of 4 M ammonium acetate.

After preparing the solutions and centrifuging the biodiesel samples, the upper phase of the centrifuged sample is removed, and 0.5 mL of the phase containing the extracted glycerol is withdrawn for analysis. Following the collection of 0.5 mL aliquots from each sample, 1.5 mL of the 1:1 (v/v) ethanol/water solution is added to serve as the reaction solvent. Subsequently, 1.2 mL of the prepared sodium periodate solution is added and agitated for 30 seconds. Then, 1.2 mL of acetylacetone is also added, and the mixture is placed in a hot water bath at 70°C for one minute. At this point, 3,5-diacetyl-1,4-dihydrolutidine is formed, and the reaction is halted by transferring the samples to a cold-water bath. Subsequently, the samples are analyzed using UV-VIS spectroscopy.

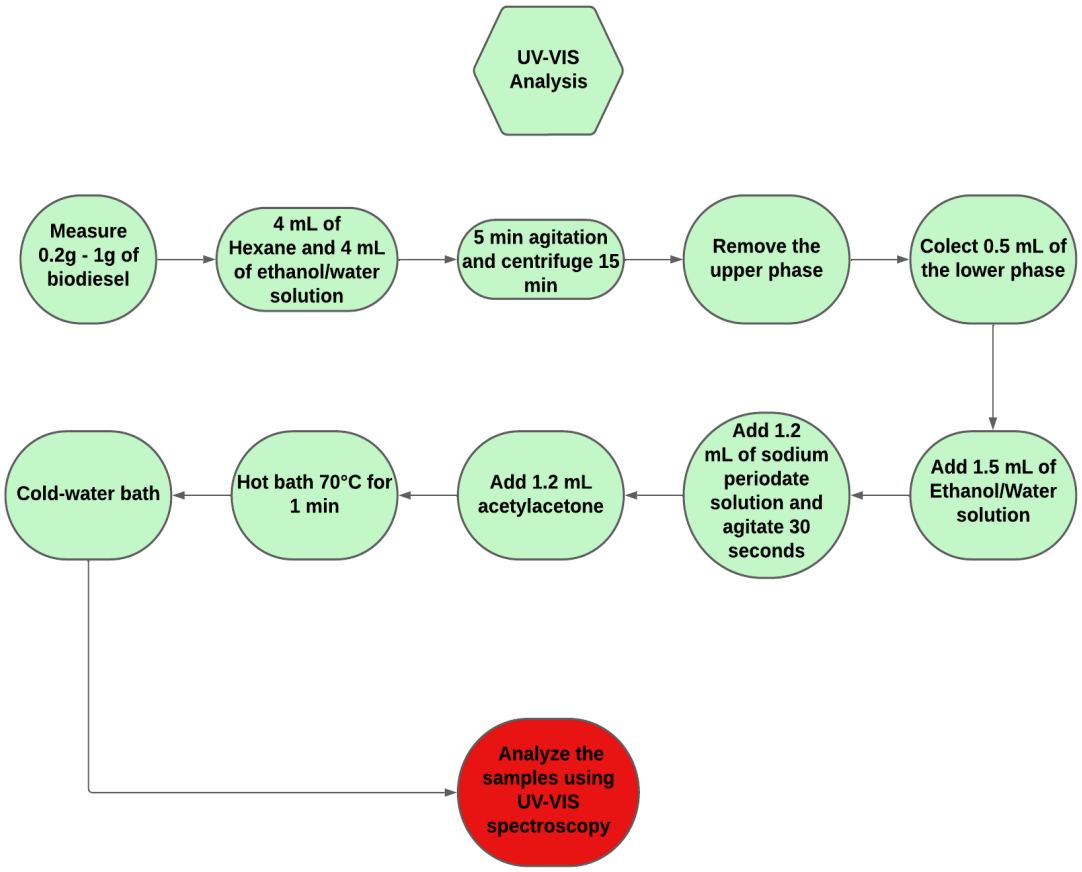

Figure 6. Methodology for quantification of glycerol using UV-Vis spectrometry after derivatization [142].

4.3 ADSORBENTS

This thesis will focus on walnut shells as the raw material for activated carbon production. The choice was made due to the abundance of walnuts in Portugal. Among dried fruits, walnuts rank third in terms of production in Portugal. Additionally, the aim is to add value to walnut shells as a waste product [143]. This section will address the three methodologies adopted for the production of the three types of charcoal.

4.3.1 Physical Activated Carbon

The initial step involved the physical activation of the precursor at 800°C in a Thermolyne muffle furnace for one hour, with a heating rate of around 10°C/min. Following activation, both samples were subjected to washing until reaching a pH of

6-7, followed by drying in an oven at 105°C for 24 hours. These washing and drying procedures were repeated for all subsequent activations conducted. After this period, physical activated carbon underwent maceration to reduce particle size.

4.3.2 H_3PO_4 Activated Carbon

For the production of chemically activated charcoal with H_3PO_4, a mass ratio of 1:1:2 was utilized for the adsorbent, acid, and water, respectively. Following the mixture, it was left in an Erlenmeyer flask for 24 hours for the impregnation phase. In the subsequent step, the sample was subjected to carbonization at 500°C for 1 hour with a heating rate of 10°C/min. Following this, the activated carbon was washed until reaching pH 7 and placed in an oven to dry for 24 hours at 105°C. After this period, the H_3PO_4 activated carbon underwent maceration to reduce particle size.

4.3.3 NaOH Activated Carbon

In the manufacturing process of chemically activated carbon with NaOH, an adsorbent-to-base-to-water mass ratio of 1:1:2 was applied. After blending the components, the mixture was allowed to undergo an impregnation phase in an Erlenmeyer flask for 24 hours. Following this, the sample underwent carbonization at 500°C for 1 hour, with a heating rate of 10°C/min. The pH of the product was adjusted to reach 7 and then dried in an oven at 105°C for 24 hours. After this period, NaOH activated carbon underwent maceration to reduce particle size.

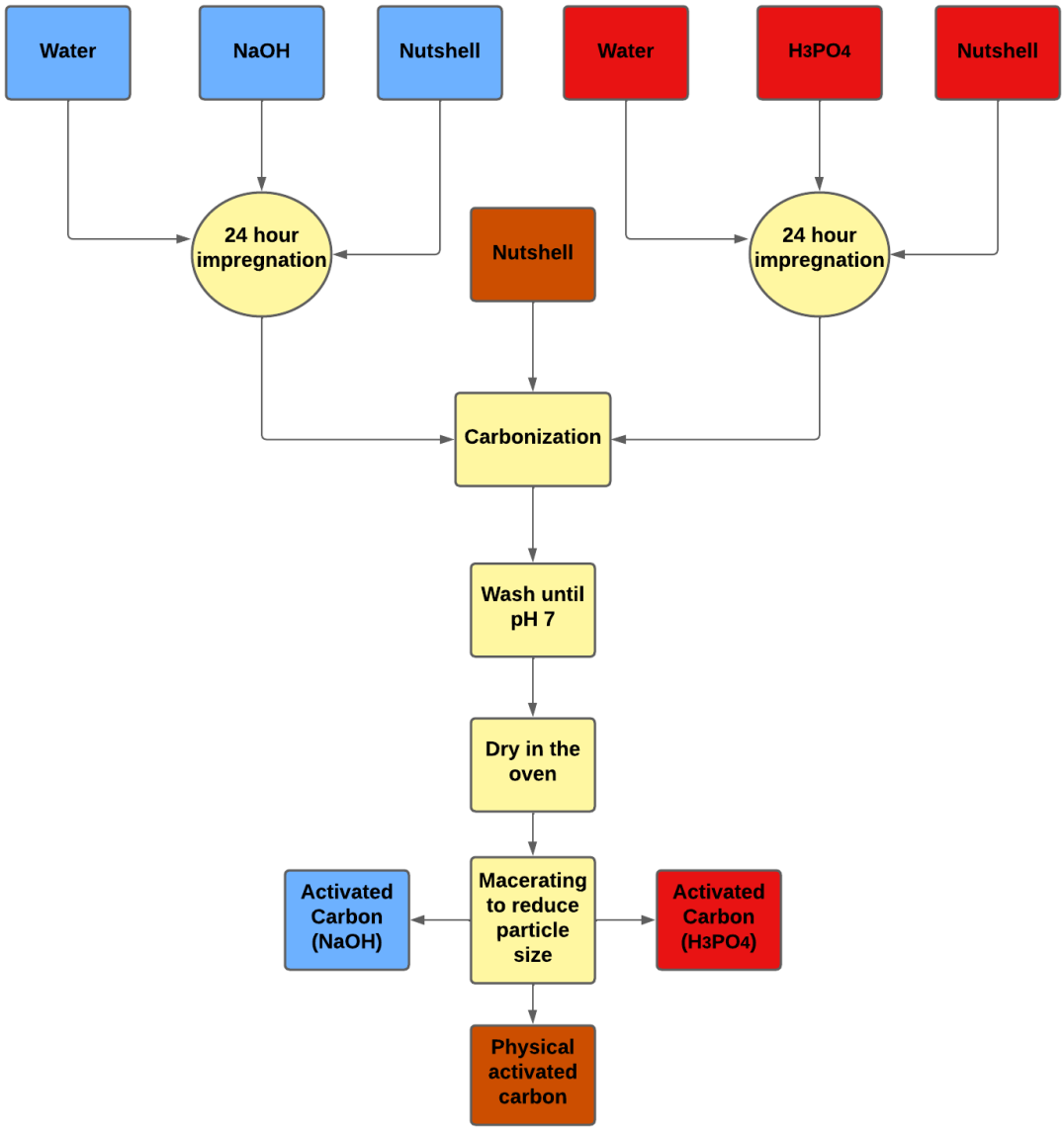

Figure 7. Preparation and activation of three different biomass-based adsorbents.

4.4 ADSORBENTS CHARACTERIZATION

4.4.1 Particle size distribution

This analysis was performed on ground walnut shells using an electromagnetic sieve shaker from the Geotechnical Laboratory of the Polytechnic Institute of Bragança (IPB). The sieves used had openings of 40, 50, 100 and 200 mesh. For this analysis, equation 7 was employed to calculate the results.

$$d_S = \frac{1}{\sum_{i=1}^{n} \frac{x_i}{D_i}} \quad (7)$$

Where:

d_S – Average Sauter diameter (mm);

x_i – Retained mass fraction;

D_i – Average opening diameter (mm).

4.4.2 Point of Zero Charge (PZC)

The determination of the point of zero charge was conducted using 10 data points. For this experiment, 10 Erlenmeyer flasks were prepared, each containing 20 mL of a NaCl solution with a concentration of 0.05 M. pH adjustments were made from 2 to 12. These adjustments were performed using 0.1 M HCl and 0.1 M NaOH solutions, with pH measurements carried out using a calibrated pH meter. Subsequently, 150 mg of the adsorbent was introduced into each flask, followed by agitation on an orbital shaker at 160 rpm for 24 hours at 20°C.

After the agitation period, the pH of the final solution in each of the 10 Erlenmeyer flasks was measured and compared with their initial pH values.

4.4.3 Textural properties

The samples underwent analysis at the *Laboratório Multiusuário de Apoio à Pesquisa do Câmpus Apucarana (LAMAP)* at the *Universidade Tecnológica Federal do Paraná*. Subsequently, the samples were subjected to degassing at 120°C for a duration of 16 hours. Surface area determination was performed utilizing the BET model (Brunauer-Emmett-Teller), while pore size distribution was assessed using the DFT method (Density Functional Theory).

4.4.4 Fourier Transform Infrared Spectroscopy (FTIR)

The Fourier transform infrared spectroscopy analysis was carried out on a PerkinElmer FTIR-ATR Spectrometer Spectrum two, as shown. Tablet samples of the adsorbents were made by combining roughly 2 mg of the substance with 200 mg KBr. The device used a range of 450 cm^{-1} to 4000 cm^{-1} to qualitatively identify functional groups in materials.

4.4.5 Thermogravimetric analysis (TGA)

The thermogravimetric analysis was conducted at the Multi-User Laboratory for Research Support (LAMAP) at Apucarana Campus, Federal Technological University of Paraná. A Thermogravimetric Analyzer TGA-50 from Shimadzu was utilized for the analysis, with Argon employed as the inert gas at a flow rate of 50 mL/min. The heating rate was set at 10 °C/min, starting from room temperature and gradually increasing until reaching 800 °C.

4.5 ADSORPTION STUDIES

For the adsorption studies the RMSE (Root Mean Square Error), was used to calculate the errors in adsorptions studies, as indicated in the three tables. The RMSE was computed using the equation provided below.

$$RMSE = \sqrt{\sum_{i=1}^{n} \frac{(\hat{y}_i - y_i)^2}{n}} \quad (8)$$

4.5.1 Adsorption kinetics

The adsorption kinetics were evaluated at three temperatures: 25°C, 35°C, and 45°C. Ten Erlenmeyer flasks were weighed with a percentage of 5% (w/w). Each flask was sampled at specific time intervals to study the behavior of the kinetic curves. The sampling times were 5, 10, 15, 30, 60, 120, 300, 360, 480, and 1440 minutes. All

analyses were performed in duplicate, and the studies were conducted using pseudo-first order, pseudo-second order, Elovich's and IPD kinetics.

4.5.2 Adsorption Isotherms

To estimate the adsorption equilibrium, experimental measurements of equilibrium adsorption isotherms were conducted. Employing a shaker incubator from Shel Lab, multiple batch experiments were carried out at the optimal temperatures identified through the kinetics analysis for each activated carbon sample. These experiments ran for 420 minutes at 160 rpm. Within 250 mL Erlenmeyer flasks, the adsorbent concentrations evaluated were 0.1%, 0.2%, 0.3%, 0.4%, 0.5%, 1%, 2%, 3%, 5%, 7%, 9% and 10% (wt/wt). Upon completion of each experiment, the adsorbent was separated from the biodiesel through filtration. Concentration analysis was conducted in duplicate. Freundlich, Sips, Liu, and Radke–Prausnitz models, were evaluated to find the best fit for the experimental data.

5 RESULTS AND DISCUSSION

5.1 BIODIESEL AND OIL CARACTERIZATION

5.1.1 Determination of acidity value

Before commencing any part of the work, it was essential to measure the acidity value of the reused cooking oil intended for biodiesel reactions. If the acidity value of the oil exceeds 2 mg KOH/g, the biodiesel would need to undergo a pretreatment with an alkaline catalyst in excess [144]. The value obtained was 0.836 ± 0.027 mg of KOH/g of crude oil, a value much lower than 2, indicating that pretreatment was unnecessary and the oil could be used for the biodiesel production.

5.1.2 Derivatization of fatty acids by BF_3

BF_3 derivatization was employed to analyze the distribution of fatty acid esters in the used waste cooking oil (WCO). The WCO sample was derivatized using BF_3 with ethanol. Subsequently, GC-FID analysis was conducted to verify the presence of the primary FAEEs in the used oil feedstock. It was observed that all the targeted FAEE compounds had been shown within 20 minutes of the chromatographic run. The weight percentage of each ester is presented in Table 14. The FAAEs were identified with the Table B1 in the Appendix B.

Table 14. Identification of fatty acids in the WCO sample.

Retention time (min)	Chemical formula	Esters	Percentage of FAEEs (wt%)
12.363	C16:0	Palmitic acid ethyl ester	10.89 ± 0.60
15.094	C18:0	Stearic acid ethyl ester	3.66 ± 0.14
15.466	C18:1n9(c+t)	Oleic acid ethyl ester, Elaidic acid ethyl ester	32.51 ± 2.56
16.264	C18:2n6(c+t)	Linoleic acid ethyl ester, Linolelaidic acid ethyl ester	47.81 ± 1.67
17.308	C18:3n3	alpha-Linolenic acid ethyl ester	5.31 ± 0.16
Total			**88.44 ± 1.86**

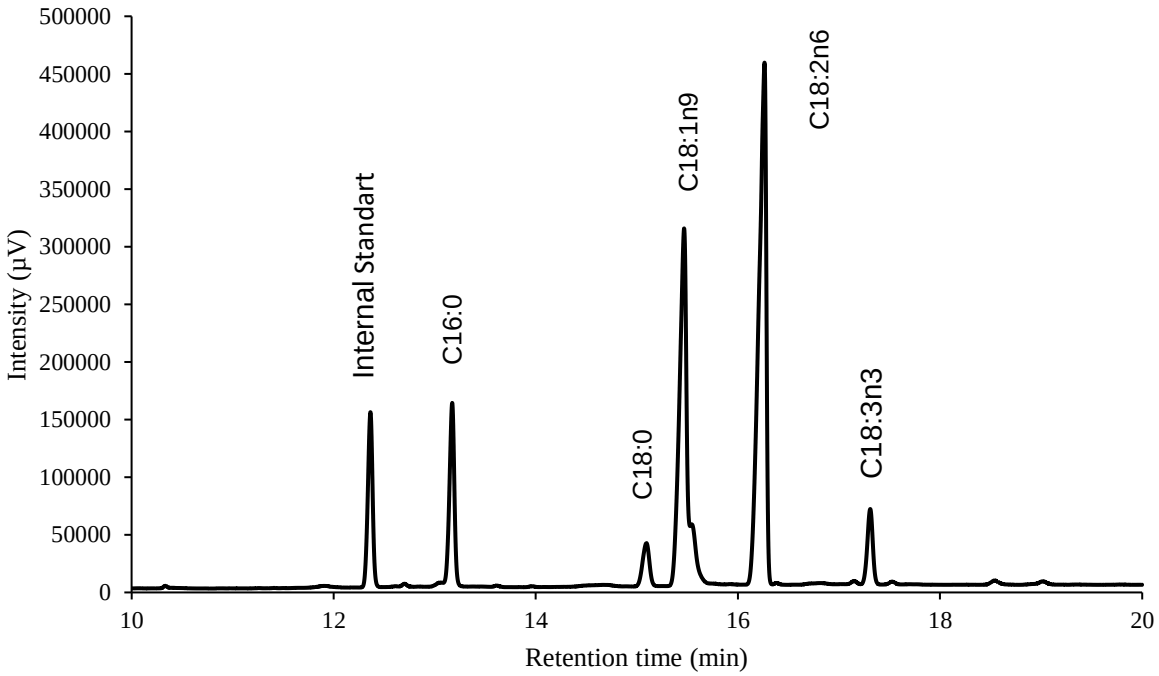

Figure 8. Identification of FAEEs in biodiesel.

By analyzing the intensity of each peak and its corresponding retention time, the identification of the FAEEs present in the biodiesel sample, and consequently, in the WCO, was feasible.

With the percentage of FAEEs and their identification, it is possible to calculate the molecular mass of the oil using the equation 5. The molecular mass of the oil obtained was 913.62 g/mol, which approximately agrees with the molecular value of sunflower oil [145].

5.1.3 Determination of FAEEs

The results of the preliminary results for the biodiesel production in large scale are presented in the Figure 9.

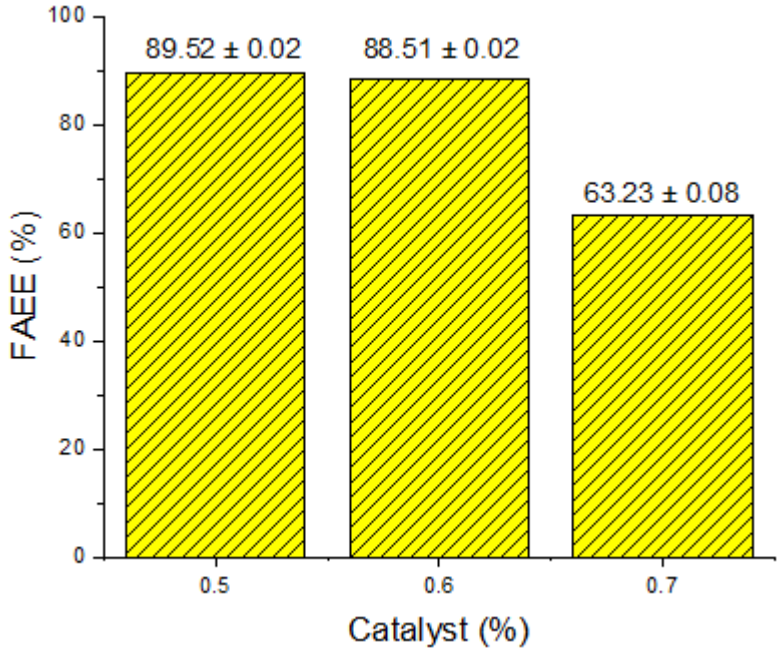

Figure 9. FAEEs mass content in the produced biodiesel.

Besides being similar with 0.6% (88.51±0.02) the result with 0.5% (89.52 ± 0.02) were slightly better with less catalyst. So, the 0.5%(wt/wt) catalyst quantity was chosen. The decrease in biodiesel conversion with increasing catalyst percentage can be attributed to the observed increase in saponification of glycerol during the decantation phase for the separation of biodiesel and glycerol phases as the catalyst concentration in the reaction medium increased.

5.1.4 Determination of reaction yield

Using Equation 6 the yield of biodiesel production was calculated with 0.5% catalyst, a molar ratio of 1:7.5 of oil/alcohol at 30°C. The reaction yield reached values of 84.57%. This result underscores the efficiency of the transesterification process under the specified conditions, indicating a substantial conversion of feedstock into biodiesel.

5.2 ADSORBENTS PRODUCTION

5.2.1 Yield of activated carbon production

The production of carbons followed the flowchart presented in Figure 6. Table 15 below shows the yield of production for the 3 carbons studied.

Table 15. Yield of activated carbon production results.

Activated Carbon	Global Yield
Physical	20.55%
H_3PO_4	59.74%
NaOH	34.86%

Chemical activation with orthophosphoric acid and sodium hydroxide results in higher carbonization yields, likely due to the lower activation temperatures used in both methods, specifically at 500°C. In contrast, the physically activated carbon demonstrated a yield of 20.55% at 800°C. This yield is deemed acceptable, especially considering that the carbonization process occurred without inert gas, resulting in greater material loss due to small amounts of oxygen in the system and also, physically activated carbon was activated at a higher temperature, which can result in the degradation of several compounds that did not occur in chemically activated carbon [122].

5.2.2 Particle size distribution

The particle size distribution of the solid was determined following the grinding of the nutshell. Table 16 displays the results, including the Sauter diameter, which corresponds to 0.1983 mm. The Sauter diameter represents the average particle diameter.

Table 16. Particle size distribution results.

Mesh	Diameter	Retained Mass (g)	Pass accumulated	% Retained
40	0.42	5.4	73.53%	26.47%
50	0.297	3.97	80.54%	19.46%
100	0.149	6.93	66.03%	33.97%
200	0.074	2.23	89.07%	10.93%
Bottom	-	1.87	0.00%	100.00%

5.2.3 Point of zero charge (pH_{PZC})

Table 17 displays the outcomes of the activated carbons produced. pH_{PZC} analyses offer insights into the surface properties of the adsorbent. Consequently,

based on the adsorbate's properties, an optimal pH for the solution can be determined, enhancing the adsorption process.

Table 17. pH_{PZC} results.

Activated Carbon	pH_{PZC}
Physical	9.59 ± 0.29
H_3PO_4	2.59 ± 0.33
NaOH	10.20 ± 0.02

The results indicated that the physically activated carbon at 800°C exhibited basic characteristics, as its pHpzc was 9.59 ± 0.29. The chemically activated carbons showed consistent results. The carbon activated with phosphoric acid had a pHpzc of 2.59 ± 0.33, and the carbon activated with sodium hydroxide had a pHpzc slightly more basic than the physically activated carbon. The value obtained was 10.20 ± 0.02

However, the pH_{PZC} analysis of each carbon may not be applicable since pH changes were not implemented in the adsorption assays. One could analyze which of the carbons had the highest glycerol removal and associate it with its pH_{PZC} result, or provide information for other researchers seeking insights into walnut shell activations and planning to implement pH changes in the studied medium. Comparing the pH_{PZC} result obtained with [2], [3], where their carbons were used for glycerol removal in biodiesel, neither of them achieved the best outcome with the most acidic carbon, as was the case in this study.

5.2.4 Textural properties

The results of the textural properties are shown in the Table 18. The analysis of surface area, micropore area, pore volume, and pore diameter indicate significant differences among the different adsorbents.

Table 18. Textural properties of the studied activated carbons.

Adsorbent	Surface area (m^2/g)	Micropore area (m^2/g)	Pore volume (cm^3/g)	Pore diameter (nm)
Physical AC	426.667	338.558	0.2236	2.4412
H_3PO_4 AC	345.689	318.422	0.1723	2.2436
NaOH AC	2.695	0.049	0.011	18.09

The physical activated carbon showed the highest surface area and micropore area, indicating a highly developed porous structure. The H_3PO_4-treated activated carbon also exhibited good properties, with a surface area of 345.7 m²/g and a micropore area of 318.4 m²/g. However, the NaOH-treated activated carbon showed very low values compared to the other two adsorbents, with a surface area of only 2.7 m²/g and a micropore area of 0.049 m²/g, indicating a significantly less developed porous structure, although your pore diameter was significantly higher than the others. This can be attributed to sodium hydroxide being a strong base, which will interact more vigorously with the surface of the adsorbent, leaving larger pores and a smaller surface area. [146] research yielded comparable results to those obtained for the NaOH-treated activated carbon based on walnut shell, with a surface area of 2.095 m²/g and a pore diameter of 32.64 nm. [147] research also demonstrated similarities to the activated carbon treated with H_3PO_4, showing a surface area of 420.5 m²/g and a pore diameter of 2.25 nm. The physically activated carbon from [148] exhibited a surface area of 368.95 m²/g and a pore diameter of 2.46 nm.

Table 19. Some textural properties of walnut activated carbons from literature.

Adsorbent	Surface area (m²/g)	Pore volume (cm³/g)	Pore diameter (nm)	References
Physical AC	368.95	0.16	2.46	[148]
H_3PO_4 AC	420.5	-	2.25	[147]
NaOH AC	2.095	-	32.64	[146]

5.2.5 Fourier Transform Infrared Spectroscopy (FTIR)

In Figure 10, the results of the FTIR analysis for the three produced carbons and also for the raw walnut shell are presented.

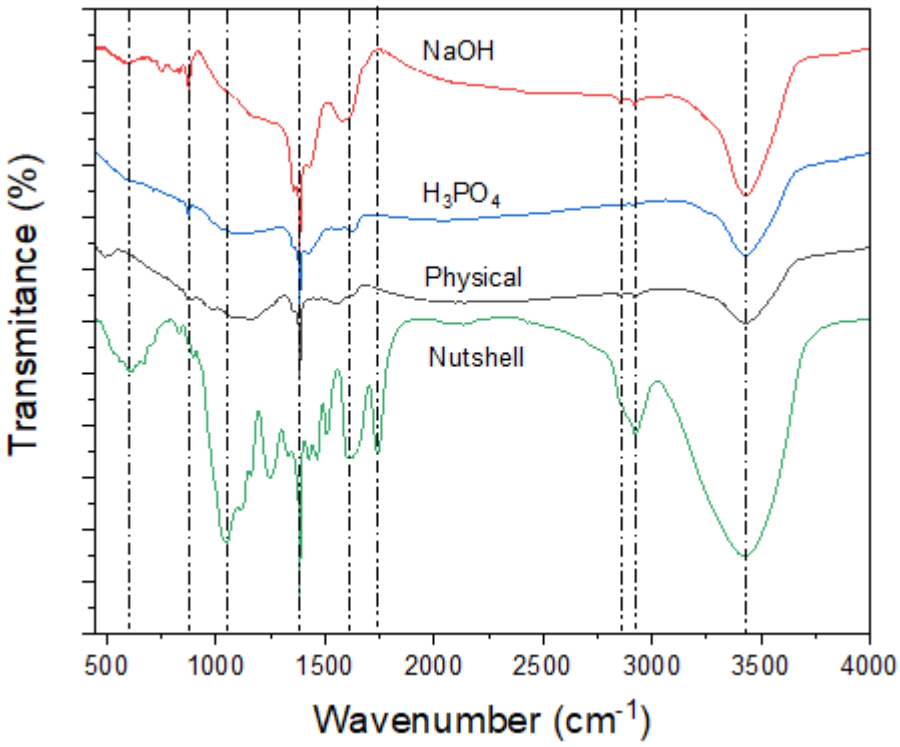

Figure 10. FTIR results for the three activated carbons and the raw material.

The bands observed at 593 cm^{-1} can be attributed to C-H vibrations occurring at the periphery of aromatic rings present in lignin. Meanwhile, the bands observed at 865 cm^{-1} may arise from N-O bending within aromatic groups, which could form during the carbonization process of the material and undergo chemical reactions with atmospheric constituents. [149]. The band in 1063 cm^{-1} can be associated with C-O deformation and cellulose aliphatic ester [150]. The band in 1386 cm^{-1} C-H vibration in plane of methyl and methylene groups [151]. The band in 1619 cm^{-1} can be attributed to vibration in aromatic ring that are found in cellulose, lignin and hemicellulose [152]. The band in 2836 cm^{-1} and 2935 cm^{-1} can be attributed to C-H vibration [149], [152] and the band in 3417 cm^{-1} is attributed to O-H stretching vibration that are presented in the lignin [149], [150], [152].

5.2.6 Thermogravimetric analysis (TGA)

The results derived from the TGA analysis are illustrated in Figure 11 alongside the first derivative curve (DTG). None of the carbons completely degraded their masses. The physical, acidic, and basic carbons experienced approximately 25%,

55%, and 60% mass loss, respectively. All carbons exhibited mass loss at around 100 °C due to moisture loss. Chemically activated carbons experienced mass loss from approximately 400°C to 600°C, attributed to the decomposition of hemicellulose, cellulose, and part of lignin. This phenomenon was particularly noticeable in the chemically activated carbons [150].

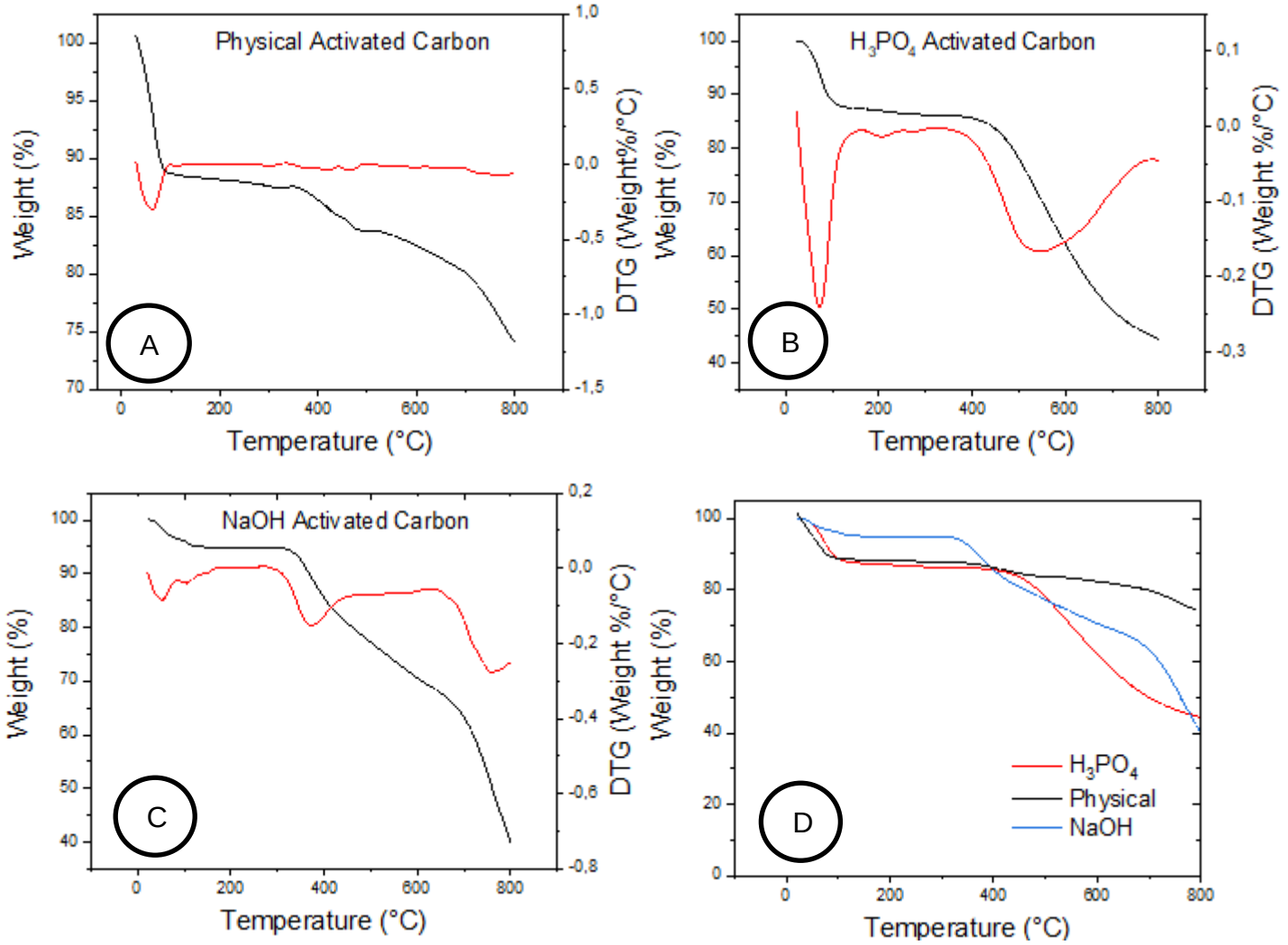

Figure 11. Thermogravimetric results of all activated carbons.

5.3 ADSORPTION STUDIES

5.3.1 Adsorption kinetics

The kinetics of adsorption were assessed across three different temperatures 25, 35 and 45°C for each of the three activated carbons prepared. Figure 12 shows the plots that were fitted for the three activated carbons and the best fitted models.

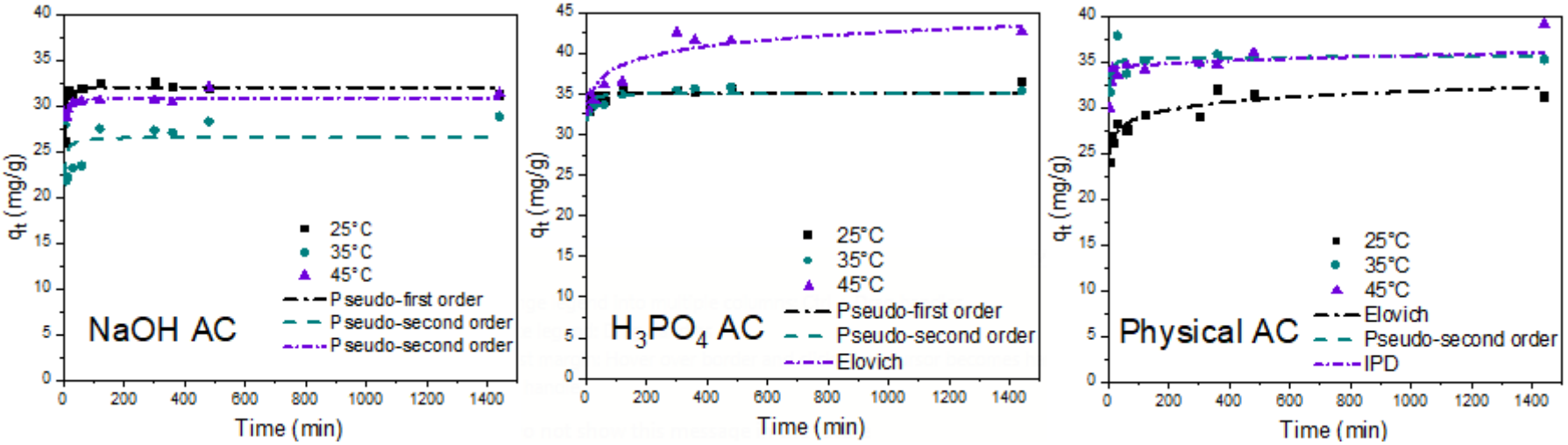

Figure 12. Kinetic plot of all activated carbons on their best fitted models.

Tables 20, 21 and 22 display the fitting parameters for the various models outlined in Chapter 3.5. All model adjustments were conducted using the OriginPro® 8.5 software.

Table 20. Kinetic data of Physical AC.

Model	T (°C)	Parameter (Unit)	Value	Standard Error	RMSE
Pseudo-first order	25	$q_e(mg\ g^{-1})$	29.51	0.6875	3.4637
		$k_1(min^{-1})$	0.2422	0.0602	
	35	$q_e(mg\ g^{-1})$	35.19	0.4293	1.5048
		$k_1(min^{-1})$	0.4021	0.0977	
	45	$q_e(mg\ g^{-1})$	35.15	0.6001	2.7833
		$k_1(min^{-1})$	0.3160	0.0815	
Pseudo-second order	25	$q_e(mg\ g^{-1})$	30.28	0.5625	1.7940
		$k_2(g\ mg^{-1}min^{-1})$	0.0207	0.0059	
	35	$q_e(mg\ g^{-1})$	35.51	0.4840	1.4782
		$k_2(g\ mg^{-1}min^{-1})$	0.0523	0.0228	
	45	$q_e(mg\ g^{-1})$	35.72	0.5964	8.5498
		$k_2(g\ mg^{-1}min^{-1})$	0.0290	0.0106	
IPD	25	$k_d(mg\ g^{-1}min^{-0.5})$	0.1833	0.0470	2.5226
		$C(mg\ g^{-1})$	26.21	0.7898	
	35	$k_d(mg\ g^{-1}min^{-0.5})$	0.0504	0.0479	8.9574
		$C(mg\ g^{-1})$	34.07	0.8051	
	45	$k_d(mg\ g^{-1}min^{-0.5})$	0.1801	0.0359	1.4731
		$C(mg\ g^{-1})$	35.05	0.6038	
Elovich	25	α $(mg\ g^{-1}min^{-1})$	1.27×10^{8}	4.10×10^{8}	1.0710
		β $(g\ mg^{-1})$	0.7982	0.1179	
	35	α $(mg\ g^{-1}min^{-1})$	3.81×10^{25}	-	4.5879
		β $(g\ mg^{-1})$	1.8403	0.0257	
	45	α $(mg\ g^{-1}min^{-1})$	1.06×10^{12}	6.68×10^{12}	6.5845
		β $(g\ mg^{-1})$	0.9305	0.1895	

Table 21. Kinetic data of H_3PO_4 AC.

Model	T (°C)	Parameter (Unit)	Value	Standard Error	RMSE
Pseudo-first order	25	$q_e(mg\ g^{-1})$	34.90	0.3098	0.8316
		$k_1(min^{-1})$	0.5507	0.1335	
	35	$q_e(mg\ g^{-1})$	34.57	0.3721	2.1891
		$k_1(min^{-1})$	0.5204	0.1439	
	45	$q_e(mg\ g^{-1})$	39.06	1.2611	11.4177
		$k_1(min^{-1})$	0.2311	0.0821	
Pseudo-second order	25	$q_e(mg\ g^{-1})$	35.29	0.2522	2.5175
		$k_2(g\ mg^{-1}min^{-1})$	0.0684	0.0194	
	35	$q_e(mg\ g^{-1})$	35.04	0.2921	1.5299
		$k_2(g\ mg^{-1}min^{-1})$	0.0553	0.0156	
	45	$q_e(mg\ g^{-1})$	40.21	1.1360	7.0092
		$k_2(g\ mg^{-1}min^{-1})$	0.0132	0.0055	
IPD	25	$k_d(mg\ g^{-1}min^{-0.5})$	0.0778	0.0166	3.5874
		$C(mg\ g^{-1})$	33.69	0.2795	
	35	$k_d(mg\ g^{-1}min^{-0.5})$	0.0865	0.0218	4.5453
		$C(mg\ g^{-1})$	33.21	0.3672	
	45	$k_d(mg\ g^{-1}min^{-0.5})$	0.1303	0.0012	3.4731
		$C(mg\ g^{-1})$	35.56	0.0335	
Elovich	25	α $(mg\ g^{-1}min^{-1})$	8.03×10^{12}	-	1.3402
		β $(g\ mg^{-1})$	0.98	0.0106	
	35	α $(mg\ g^{-1}min^{-1})$	3.41×10^{22}	2.31×10^{23}	6.1685
		β $(g\ mg^{-1})$	1.65	0.2007	
	45	α $(mg\ g^{-1}min^{-1})$	4.22×10^{10}	4.67×10^{10}	2.0083
		β $(g\ mg^{-1})$	0.7850	0.0294	

Table 22. Kinetic data of NaOH AC.

Model	T (°C)	Parameter (Unit)	Value	Standard Error	RMSE
Pseudo-first order	25	$q_e(mg\ g^{-1})$	31.97	0.1645	2.2161
		$k_1(min^{-1})$	0.3477	0.0311	
	35	$q_e(mg\ g^{-1})$	26.64	0.8172	4.4021
		$k_1(min^{-1})$	0.1336	0.0313	
	45	$q_e(mg\ g^{-1})$	30.46	0.3149	7.8731
		$k_1(min^{-1})$	0.6307	0.1972	
Pseudo-second order	25	$q_e(mg\ g^{-1})$	32.40	0.3406	4.7225
		$k_2(g\ mg^{-1}min^{-1})$	0.0379	0.0095	
	35	$q_e(mg\ g^{-1})$	27.57	0.6330	1.9266
		$k_2(g\ mg^{-1}min^{-1})$	0.0098	0.0025	
	45	$q_e(mg\ g^{-1})$	30.84	0.2726	2.4692
		$k_2(g\ mg^{-1}min^{-1})$	0.0809	0.0289	
IPD	25	$k_d(mg\ g^{-1}min^{-0.5})$	0.0558	0.0561	3.5958
		$C(mg\ g^{-1})$	30.55	0.9428	
	35	$k_d(mg\ g^{-1}min^{-0.5})$	0.2124	0.0488	6.4119
		$C(mg\ g^{-1})$	22.49	0.8632	
	45	$k_d(mg\ g^{-1}min^{-0.5})$	0.0641	0.0192	1.4217
		$C(mg\ g^{-1})$	29.51	0.0322	
Elovich	25	α $(mg\ g^{-1}min^{-1})$	6.88×10^{20}	1.77×10^{22}	2.6638
		β $(g\ mg^{-1})$	1.6911	0.8255	
	35	α $(mg\ g^{-1}min^{-1})$	1.54×10^{5}	2.82×10^{5}	5.8063
		β $(g\ mg^{-1})$	0.6353	0.0759	
	45	α $(mg\ g^{-1}min^{-1})$	2.17×10^{28}	4.67×10^{29}	9.2769
		β $(g\ mg^{-1})$	0.7850	0.0294	

Among the selected models, all presented low value of RMSE. One possible reason for this could be the choice of analysis times, which were closely spaced, making it easier for the curve to fit the initial data points. As the temperature increased for all three carbons, there was an improvement in glycerol removal. In the phosphoric

acid activated carbon, a significant increase in equilibrium adsorption capacity (q_e) was observed from 35°C to 45°C. For the physically activated carbon, there was a positive change in q_e value from 25°C to 35°C, with a similar value maintained at 45°C. In contrast, for the NaOH activated carbon, the values did not change to the same extent with increasing temperature, although an improvement in q_e value was observed.

The influence of temperature on adsorption processes is multifaceted. As temperature rises, there is an augmentation in adsorption attributed to various factors. Firstly, the increase in temperature leads to a rise in the number of active surface sites available for adsorption on each adsorbent, alongside enhancing porosity and total pore volume. Additionally, the decrease in the thickness of the boundary layer surrounding the sorbent contributes to this enhancement, reducing the mass transfer resistance of adsorbate. Additionally, temperature adjustments induce changes in the equilibrium capacity of the adsorbent for a specific adsorbate. Simultaneously, increasing temperature accelerates the diffusion rate of adsorbate molecules across both the external boundary layer and the internal pores of the adsorbent particle, facilitated by the decrease in solution viscosity [153], [154]. For the study of activation energies, Table 23 presents the results of the linearization used according to Equation 3.

Table 23. Activation energy for the three activated carbons.

AC	Model	Ea (kJ/mol)	R^2
Physical	Pseudo-first order	10.7929	0.2920
	Pseudo-second order	13.9236	0.1420
H_3PO_4	Pseudo-first order	-33.8730	0.7834
	Pseudo-second order	-64.2656	0.8313
NaOH	Pseudo-first order	22.3811	0.1317
	Pseudo-second order	28.3840	0.1136

For the physically activated carbon, the activation energy (Ea) values calculated for the pseudo-first and pseudo-second order models are 10.7929 kJ/mol and 13.9236 kJ/mol, respectively. These relatively low activation energy values indicate that the adsorption process is predominantly governed by physical interactions rather than chemical reactions. However, it's noteworthy that both models exhibit relatively low coefficients of determination (R^2), suggesting that the experimental data may not fit perfectly with the theoretical models.

In contrast, the NaOH activated carbon demonstrates higher activation energy values for both the pseudo-first order (22.3811 kJ/mol) and pseudo-second order (28.3840 kJ/mol) models. This indicates that the adsorption process on NaOH activated carbon involves stronger interactions, possibly indicating a combination of physical and chemical adsorption mechanisms. Despite the higher activation energy values, the R^2 values for both models remain low, implying that the experimental data may not be fully explained by the kinetic models [155].

For the H_3PO_4 activated carbon, the activation energy was determined to be negative. While a negative activation energy value doesn't have physical meaning, according to the Arrhenius equation, for the value to be negative, the rate constant (k), which represents the adsorption rate, must decrease as the temperature increases. This behavior was observed in the k values obtained for the H_3PO_4 activated carbon [156].

Overall, while the activation energy values provide insights into the nature of the adsorption process, the relatively low coefficients of determination suggest that the adsorption kinetics of these activated carbons may be influenced by other factors not accounted for in the kinetic models. Further investigation may be necessary to fully explain the adsorption mechanisms at play in these systems.

5.3.2 Adsorption Isotherms

The investigation of equilibrium adsorption isotherms was conducted at optimal temperatures identified in the kinetics studies. For the physical AC, H_3PO_4 AC and NaOH AC the better temperatures were 35°C, 45°C and 25°C. Utilizing adsorbent concentrations ranging from 0.1 to 10% by mass. Experimental data points along with adjustments using four equation models are depicted in Figures 13 for analysis. Fitting of the data was performed using Origin Pro® 8.5 software.

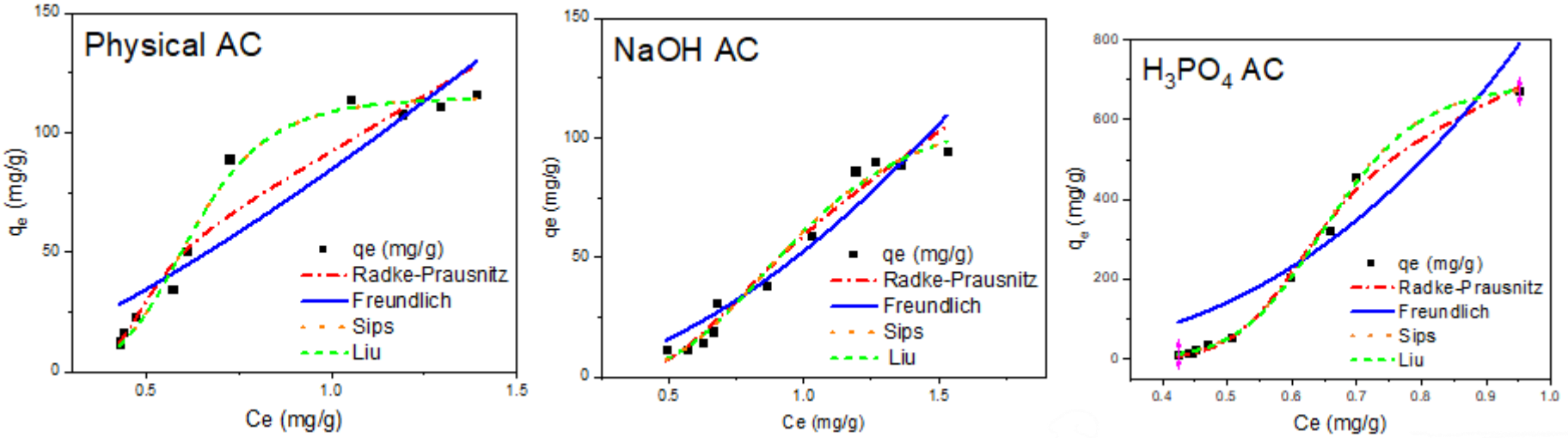

Figure 13. Isotherm plot for the three activated carbons in their best kinetics temperatures results.

The Table 24 presents the parameters adjusted for each isotherm and its present activated carbon.

Table 24. Isotherm data of all activated carbons on their best kinetics temperatures.

Model	AC	Parameter	Value	Standard Error	RMSE
Freundlich	Physical	$K_f\ (mg\ g^{-1})(mg\ g^{-1})^{-1/n_f}$	84.71	6.2451	302.4862
		n_f	0.5654	0.1319	
	H_3PO_4	$K_f\ (mg\ g^{-1})(mg\ g^{-1})^{-1/n_f}$	834.85	105.0723	7033.22
		n_f	0.3459	0.0532	
	NaOH	$K_f\ (mg\ g^{-1})(mg\ g^{-1})^{-1/n_f}$	52.64	3.5256	92.8422
		n_f	0.5820	0.0706	
Sips	Physical	$q_s\ (mg\ g^{-1})$	115.05	3.1940	28.0723
		$K_s\ (g\ mg^{-1})^{n_s}$	17.1489	7.2123	
		n_s	5.9915	0.6952	
	H_3PO_4	$q_s\ (mg\ g^{-1})$	696.79	14.3240	130.4741
		$K_s\ (g\ mg^{-1})^{n_s}$	47.0510	11.6994	
		n_s	9.2423	0.5000	
	NaOH	$q_s\ (mg\ g^{-1})$	114.7375	14.3366	32.1447
		$K_s\ (g\ mg^{-1})^{n_s}$	1.1318	0.4093	
		n_s	3.9372	0.6588	
Radke-Prausnitz	Physical	$a\ (\mathrm{g/mg})$	92.2899	4.8597	148.6584
		$b\ [(mg\ g^{-1})/(mg\ g^{-1})^m]]$	$7.05\text{x}10^4$	$3.79\text{x}10^5$	
		m	9.77	5.8437	
	H_3PO_4	$a\ (\mathrm{g/mg})$	720.2381	20.0203	321.4113
		$b\ [(mg\ g^{-1})/(mg\ g^{-1})^m]$	$1.66\text{x}10^5$	$1.03\text{x}10^5$	
		m	11.56	1.2002	
	NaOH	$a\ (\mathrm{g/mg})$	68.8733	5.3358	48.0133
		$b\ [(mg\ g^{-1})/(mg\ g^{-1})^m]$	430.5500	367.1998	
		m	5.59	1.8911	
Liu	Physical	$q_{liu}\ (mg\ g^{-1})$	115.0454	3.1824	28.0723
		$K_{liu}\ (mg\ g^{-1})$	1.6069	0.0370	
		n_{liu}	5.9935	0.6852	
	H_3PO_4	$q_{liu}\ (mg\ g^{-1})$	696.7986	14.2483	130.4742
		$K_{liu}\ (mg\ g^{-1})$	1.5169	0.0106	
		n_{liu}	9.2431	0.4869	
	NaOH	$q_{liu}\ (mg\ g^{-1})$	114.7428	14.3323	32.1447
		$K_{liu}\ (mg\ g^{-1})$	1.0319	0.0900	
		n_{liu}	3.9369	0.6618	

All selected isotherms were effectively fitted to the data, exhibiting favorable values of RMSE. The initial choice among these models was the Freundlich isotherm. The Freundlich adsorption isotherm model is utilized to depict reversible and non-ideal adsorption processes. Its expression delineates the surface's heterogeneity, along with the exponential distribution of active sites and their corresponding energies [136].

The subsequent selection involved the Sips model, derived from a combination of the Langmuir and Freundlich isotherm models. The Sips isotherm model was developed to account for the heterogeneity observed in adsorption systems and to address the constraints associated with high concentrations of adsorbate encountered in the Freundlich model. Consequently, this formulation provides a finite limit at elevated concentrations. Likewise, both the Freundlich and Sips models exhibit certain limitations, particularly in failing to accurately predict Henry's law behavior at low pressures. Notably, the Sips model demonstrated the most favorable fit among the isotherms considered in this study [136].

The Liu model was selected due to its combination of Freundlich and Langmuir isotherms, similar to the Sips model. Consequently, the models overlapped each other in the observed isotherm graphs. The authors [3], [157] observed the same results as this work

The Radke-Prausnitz model was selected as the last model for fitting the experimental data. In 1972, researchers applied this model to elucidate the adsorption characteristics of micropollutants, including p-cresol and p-chlorophenol, onto activated carbon. Despite the study's primary focus not being on micropollutants, the Radke-Prausnitz isotherm yielded a notable value of RMSE, accentuating its efficacy in accurately representing the experimental data [138].

5.3.3 Glycerol removal

For the studies of glycerol removal, the adsorption kinetics results were analyzed for the three temperatures described in the kinetic methodology of this work and for the three types of activated carbons.

Figure 14 shows the glycerol removal in the kinetic analyses with 5% (wt/wt) of biodiesel for the adsorbent.

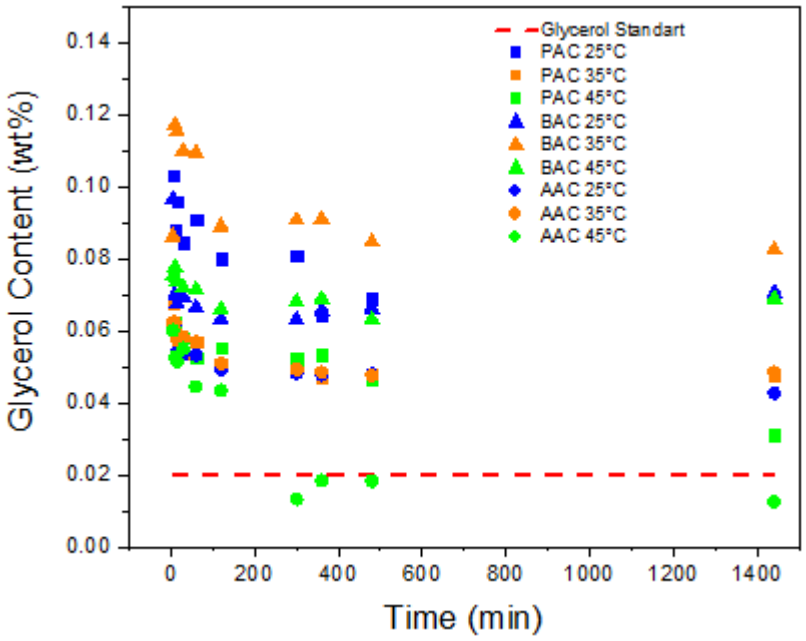

Figure 14. Glycerol removal in the kinetics studies for all the three AC in 25°C, 35°C and 45°C.

According to the graph, only the activated carbon treated with phosphoric acid at 45°C and a concentration of 5% (wt/wt) met the glycerol removal standards set by EN 14214 and ASTM D6751. The process stabilized at approximately 300 minutes, resulting in a glycerol removal percentage of 0.0125%. For the basic activated carbon, the most effective removal occurred at 25°C, achieving a glycerol removal percentage of 0.0629% at 300 minutes. In the case of the physical activated carbon, the highest removal efficiency was observed after 24 hours, with a glycerol removal percentage of 0.0310% in the biodiesel sample.

6. CONCLUSIONS AND FUTURE WORKS

Biodiesel serves as a renewable and environmentally friendly alternative for utilization in transportation vehicles and related sectors. Various methods and raw materials can be employed in the production of biodiesel, and in this study, the transesterification reaction was conducted utilizing waste cooking oil as the feedstock. This approach not only provides an alternative to fossil fuel diesel but also offers a sustainable solution for managing a common residue. Various characterizations of the oil and biodiesel were conducted, considering the molar mass equivalent to 913.62 g/mol. Following the determination of the molar mass of the oil used, the parameter identified in a preliminary analysis for achieving the highest conversion into biodiesel was a catalyst percentage of 0.5%. Subsequently, biodiesel production was carried out under the parameters of 30°C and an oil/alcohol molar ratio of 1:7.5.

In order to achieve the target glycerol percentage of 0.02% (w/w) in accordance with EN 14214/ASTM D6751 standards, three activated carbons were prepared for adsorption assays. All carbons exhibited an affinity for glycerol adsorption; however, only the phosphoric acid activated carbon at 45°C proved effective with dry washing to meet the standards, reaching 0.0125% glycerol content, which is 37.5% below the limit required by both European and American standards. Activated carbons prepared with phosphoric acid, sodium hydroxide, and physical activation yielded promising results in terms of surface area characterization and pore diameters, consistent with literature findings.

Based on the findings, it can be concluded that the adsorption process has the potential to serve as a substitute for the conventional wet washing method. The methodology of dry washing was found to achieve comparable levels of purity in biodiesel. However, the minimum esters content value of 96.5 (wt.%) required for biodiesel was not reached. This discrepancy does not result from an ineffective purification process, it is likely attributed to the presence of unreacted triglycerides and the source of the oil that is not a “clean” oil. Addressing those issues may necessitate further investigation into the transesterification reaction of the waste oil.

For future research purposes, it may be worthwhile to investigate the initial treatment of used cooking oil through esterification reaction, followed by transesterification, to achieve the minimum esters limit in biodiesel. Additionally,

exploring the replacement of the catalyst utilized in this study with heterogeneous acidic and basic catalysts, as well as homogeneous acidic catalysts, could provide insights into whether the conversion of oil to biodiesel yields improved outcomes. Furthermore, column adsorption studies could be conducted to ascertain if glycerol removal rates are higher. In this study, only one of the activated carbons, at a specific temperature, met the standard through dry washing.

REFERENCES

[1] S. Dey, N. M. Reang, P. K. Das, and M. Deb, “A comprehensive study on prospects of economy, environment, and efficiency of palm oil biodiesel as a renewable fuel,” *J Clean Prod*, vol. 286, pp. 124–981, 2021, doi: 10.1016/j.jclepro.2020.124981.

[2] M. Garção, “BIODIESEL PRODUCTION FROM RESIDUAL COOKING OILS AND PURIFICATION BY ADSORPTION PROCESSES BASED ON ADSORBENTS OF NATURAL ORIGIN,” 2023.

[3] G. Lamino Camilo, “PRODUCTION OF ETHANOLIC BIODIESEL FROM WASTE COOKING OILS AND PURIFICATION THROUGH ADSORPTION USING OLIVE PITS BASED MATERIALS,” 2023.

[4] A. H. Tesfay, S. H. Asfaw, and M. G. Bidir, “Comparative evaluation of biodiesel production and engine characteristics of Jatropha and Argemone Mexicana oils,” *SN Appl Sci*, vol. 1, no. 9, pp. 1–12, 2019, doi: 10.1007/s42452-019-1075-2.

[5] Z. Hu *et al.*, “Waste cooking oil biodiesel and petroleum diesel soot from diesel bus: A comparison of morphology, nanostructure, functional group composition and oxidation reactivity,” *Fuel*, vol. 321, no. February, p. 124019, 2022, doi: 10.1016/j.fuel.2022.124019.

[6] A. Al-Saadi, B. Mathan, and H. Yinghe, “Biodiesel production via simultaneous transesterification and esterification reactions over SrO–ZnO/Al2O3 as a bifunctional catalyst using high acidic waste cooking oil,” *Chemical Engineering Research and Desing* , 2020.

[7] M. V. Rodionova *et al.*, “Biofuel production: Challenges and opportunities,” *Int J Hydrogen Energy*, vol. 42, no. 12, pp. 8450–8461, 2017, doi: 10.1016/j.ijhydene.2016.11.125.

[8] X. Ma *et al.*, “Current application of MOFs based heterogeneous catalysts in catalyzing transesterification/esterification for biodiesel production: A review,” *Energy Convers Manag*, vol. 229, no. December 2020, pp. 113–760, 2021, doi: 10.1016/j.enconman.2020.113760.

[9] I. Thushari and S. Babel, “Biodiesel Production from Waste Palm Cooking Oil Using Solid Acid Catalyst Derived from Coconut Meal Residue,” *Waste*

Biomass Valorization, vol. 11, no. 9, pp. 4941–4956, 2020, doi: 10.1007/s12649-019-00820-9.

[10] R. Ahmed and K. Huddersman, “Review of biodiesel production by the esterification of wastewater containing fats oils and grease (FOGs),” *Journal of Industrial and Engineering Chemistry*, vol. 110, pp. 1–14, 2022, doi: 10.1016/j.jiec.2022.02.045.

[11] S. Ameer and K. R. Gopal, “A review of the effects of catalyst and additive on biodiesel production , performance , combustion and emission characteristics,” *Renewable and Sustainable Energy Reviews*, vol. 16, no. 1, pp. 711–717, 2012, doi: 10.1016/j.rser.2011.08.036.

[12] J. I. Orege *et al.*, *Recent advances in heterogeneous catalysis for green biodiesel production by transesterification*, vol. 258, no. March. Elsevier Ltd, 2022. doi: 10.1016/j.enconman.2022.115406.

[13] M. C. Hsiao, J. Y. Kuo, S. A. Hsieh, P. H. Hsieh, and S. S. Hou, “Optimized conversion of waste cooking oil to biodiesel using modified calcium oxide as catalyst via a microwave heating system,” *Fuel*, vol. 266, no. July 2019, p. 117114, 2020, doi: 10.1016/j.fuel.2020.117114.

[14] B. Thangaraj, P. R. Solomon, B. Muniyandi, S. Ranganathan, and L. Lin, “Catalysis in biodiesel production - A review,” *Clean Energy*, vol. 3, no. 1, pp. 2–23, 2019, doi: 10.1093/ce/zky020.

[15] S. Semwal, A. K. Arora, R. P. Badoni, and D. K. Tuli, “Biodiesel production using heterogeneous catalysts,” *Bioresour Technol*, vol. 102, no. 3, pp. 2151–2161, 2011, doi: 10.1016/j.biortech.2010.10.080.

[16] I. F. Nata, M. D. Putra, C. Irawan, and C. K. Lee, “Catalytic performance of sulfonated carbon-based solid acid catalyst on esterification of waste cooking oil for biodiesel production,” *J Environ Chem Eng*, vol. 5, no. 3, pp. 2171–2175, 2017, doi: 10.1016/j.jece.2017.04.029.

[17] N. Mansir, Y. H. Taufiq-Yap, U. Rashid, and I. M. Lokman, “Investigation of heterogeneous solid acid catalyst performance on low grade feedstocks for biodiesel production: A review,” *Energy Convers Manag*, vol. 141, pp. 171–182, 2017, doi: 10.1016/j.enconman.2016.07.037.

[18] R. Leesing, S. Siwina, and K. Fiala, “Yeast-based biodiesel production using sulfonated carbon-based solid acid catalyst by an integrated biorefinery of

durian peel waste," *Renew Energy*, vol. 171, pp. 647–657, 2021, doi: 10.1016/j.renene.2021.02.146.

[19] L. R. V. da Conceição, L. M. Carneiro, J. D. Rivaldi, and H. F. de Castro, "Solid acid as catalyst for biodiesel production via simultaneous esterification and transesterification of macaw palm oil," *Ind Crops Prod*, vol. 89, pp. 416–424, 2016, doi: 10.1016/j.indcrop.2016.05.044.

[20] F. Esmi, V. B. Borugadda, and A. K. Dalai, "Heteropoly acids as supported solid acid catalysts for sustainable biodiesel production using vegetable oils: A review," *Catal Today*, vol. 404, no. December 2021, pp. 19–34, 2022, doi: 10.1016/j.cattod.2022.01.019.

[21] I. M. Rizwanul Fattah *et al.*, "State of the Art of Catalysts for Biodiesel Production," *Front Energy Res*, vol. 8, no. June, pp. 1–17, 2020, doi: 10.3389/fenrg.2020.00101.

[22] M. Alshari and H. Znad, "Transesteri fi cation of waste canola oil by lithium / zinc composite supported on waste chicken bone as an effective catalyst," vol. 151, pp. 740–749, 2020.

[23] K. Nomura, P. Terwilliger, A. V. S. L. S. Bharadwaj, M. Singh, S. Niju, and K. M. M. S. Begum, "Self-dual Leonard pairs Biodiesel production from rubber seed oil using calcium oxide derived from eggshell as catalyst – optimization and modeling studies a," pp. 430–442, 2019.

[24] M. Kouzu, T. Kasuno, M. Tajika, Y. Sugimoto, S. Yamanaka, and J. Hidaka, "Calcium oxide as a solid base catalyst for transesterification of soybean oil and its application to biodiesel production," *Fuel*, vol. 87, no. 12, pp. 2798–2806, 2008.

[25] Y. Hua, M. Omar, J. Kansedo, N. Mujawar, Y. San, and C. Nolasco-hipolito, "Biodiesel production from used cooking oil using green solid catalyst derived from calcined fusion waste chicken and fi sh bones," *Renew Energy*, vol. 139, no. November 2014, pp. 696–706, 2019, doi: 10.1016/j.renene.2019.02.110.

[26] B. K. Uprety, W. Chaiwong, C. Ewelike, and S. K. Rakshit, "Biodiesel production using heterogeneous catalysts including wood ash and the importance of enhancing byproduct glycerol purity," *Energy Convers Manag*, vol. 115, pp. 191–199, 2016, doi: 10.1016/j.enconman.2016.02.032.

[27] P. Nair, B. Singh, S. N. Upadhyay, and Y. C. Sharma, “Synthesis of biodiesel from low FFA waste frying oil using calcium oxide derived from Mereterix mereterix as a heterogeneous catalyst,” *J Clean Prod*, vol. 29–30, pp. 82–90, 2012, doi: 10.1016/j.jclepro.2012.01.039.

[28] B. A. V. S. L. Sai, N. Subramaniapillai, K. Mohamed, M. Sheriffa, and A. Narayanan, “Journal of Environmental Chemical Engineering Optimization of continuous biodiesel production from rubber seed oil (RSO) using calcined eggshells as heterogeneous catalyst,” vol. 8, no. December 2019, 2020, doi: 10.1016/j.jece.2019.103603.

[29] H. Mahmood Khan, T. Iqbal, C. Haider Ali, A. Javaid, and I. Iqbal Cheema, “Sustainable biodiesel production from waste cooking oil utilizing waste ostrich (Struthio camelus) bones derived heterogeneous catalyst,” *Fuel*, vol. 277, no. April, p. 118091, 2020, doi: 10.1016/j.fuel.2020.118091.

[30] A. N. Amenaghawon, K. Obahiagbon, V. Isesele, and F. Usman, “Optimized biodiesel production from waste cooking oil using a functionalized bio-based heterogeneous catalyst,” *Clean Eng Technol*, vol. 8, no. May, p. 100501, 2022, doi: 10.1016/j.clet.2022.100501.

[31] R. Naveenkumar and G. Baskar, “Biodiesel production from Calophyllum inophyllum oil using zinc doped calcium oxide (Plaster of Paris) nanocatalyst,” *Bioresour Technol*, vol. 280, no. January, pp. 493–496, 2019, doi: 10.1016/j.biortech.2019.02.078.

[32] A. L. De Lima, C. M. Ronconi, and C. J. A. Mota, “Heterogeneous basic catalysts for biodiesel production,” *Catal Sci Technol*, vol. 6, no. 9, pp. 2877–2891, 2016, doi: 10.1039/c5cy01989c.

[33] M. Ramos, A. P. Soares Dias, J. F. Puna, J. Gomes, and J. C. Bordado, “Biodiesel Production Processes and Sustainable Raw Materials,” *Energies (Basel)*, 2019.

[34] S. K. Karmee and A. Chadha, “Preparation of biodiesel from crude oil of Pongamia pinnata,” *Bioresour Technol*, vol. 96, no. 13, pp. 1425–1429, 2005, doi: 10.1016/j.biortech.2004.12.011.

[35] L. C. Meher, V. S. S. Dharmagadda, and S. N. Naik, “Optimization of alkali-catalyzed transesterification of Pongamia pinnata oil for production of

biodiesel," *Bioresour Technol*, vol. 97, no. 12, pp. 1392–1397, 2006, doi: 10.1016/j.biortech.2005.07.003.

[36] J. M. Dias, M. C. M. Alvim-Ferraz, and M. F. Almeida, "Comparison of the performance of different homogeneous alkali catalysts during transesterification of waste and virgin oils and evaluation of biodiesel quality," *Fuel*, vol. 87, no. 17–18, pp. 3572–3578, 2008, doi: 10.1016/j.fuel.2008.06.014.

[37] Sahar *et al.*, "Biodiesel production from waste cooking oil: An efficient technique to convert waste into biodiesel," *Sustain Cities Soc*, vol. 41, no. May, pp. 220–226, 2018, doi: 10.1016/j.scs.2018.05.037.

[38] O. Alamu, M. Waheed, S. Jekayinfa, and T. Akintola, "Optimal Transesterification Duration for Biodiesel Production from Nigerian Palm Kernel Oil," *Agricultural Engineering International: the CIGR Ejournal*, vol. 9, pp. 1–11, 2007.

[39] H. J. Berchmans, K. Morishita, and T. Takarada, "Kinetic study of hydroxide-catalyzed methanolysis of Jatropha curcas-waste food oil mixture for biodiesel production," *Fuel*, vol. 104, pp. 46–52, 2013, doi: 10.1016/j.fuel.2010.01.017.

[40] B. S. Gandhi, S. S. Chelladurai, and D. S. Kumaran, "Process Optimization for Biodiesel Synthesis From Jatropha Curcas Oil," *Distributed Generation & Alternative Energy Journal*, vol. 26, no. 4, pp. 6–16, Sep. 2011, doi: 10.1080/21563306.2011.10462201.

[41] Y. C. Sharma and B. Singh, "A hybrid feedstock for a very efficient preparation of biodiesel," *Fuel Processing Technology*, vol. 91, no. 10, pp. 1267–1273, 2010, doi: 10.1016/j.fuproc.2010.04.008.

[42] A. Kumar and S. Sharma, "Potential non-edible oil resources as biodiesel feedstock: An Indian perspective," *Renewable and Sustainable Energy Reviews*, vol. 15, no. 4, pp. 1791–1800, 2011, doi: 10.1016/j.rser.2010.11.020.

[43] S. V. Ghadge and H. Raheman, "Process optimization for biodiesel production from mahua (Madhuca indica) oil using response surface methodology," *Bioresour Technol*, vol. 97, no. 3, pp. 379–384, 2006, doi: 10.1016/j.biortech.2005.03.014.

[44] R. Sathish Kumar, K. Sureshkumar, and R. Velraj, "Optimization of biodiesel production from Manilkara zapota (L.) seed oil using Taguchi method," *Fuel*, vol. 140, no. x, pp. 90–96, 2015, doi: 10.1016/j.fuel.2014.09.103.

[45] J. Y. Kenneth, “The Optimization of Alkali-Catalyzed Biodiesel Production from Camelina sativa Oil Using a Response Surface Methodology,” *J Bioprocess Biotech*, vol. 05, no. 07, 2015, doi: 10.4172/2155-9821.1000235.

[46] U. Rashid and F. Anwar, “Production of biodiesel through optimized alkaline-catalyzed transesterification of rapeseed oil,” *Fuel*, vol. 87, no. 3, pp. 265–273, 2008, doi: 10.1016/j.fuel.2007.05.003.

[47] D. O. Onukwuli, L. N. Emembolu, C. N. Ude, S. O. Aliozo, and M. C. Menkiti, “Optimization of biodiesel production from refined cotton seed oil and its characterization,” *Egyptian Journal of Petroleum*, vol. 26, no. 1, pp. 103–110, 2017, doi: 10.1016/j.ejpe.2016.02.001.

[48] M. Anwar, M. G. Rasul, and N. Ashwath, “Production optimization and quality assessment of papaya (Carica papaya) biodiesel with response surface methodology,” *Energy Convers Manag*, vol. 156, no. November 2017, pp. 103–112, 2018, doi: 10.1016/j.enconman.2017.11.004.

[49] A. Parlak, H. Karabas, V. Ayhan, H. Yasar, H. S. Soyhan, and I. Ozsert, “Comparison of the Variables Affecting the Yield of Tobacco Seed Oil Methyl Ester for KOH and NaOH Catalysts,” *Energy & Fuels*, vol. 23, no. 4, pp. 1818–1824, Apr. 2009, doi: 10.1021/ef800371g.

[50] A. S. Silitonga *et al.*, “Schleichera oleosa L oil as feedstock for biodiesel production,” *Fuel*, vol. 156, pp. 63–70, 2015, doi: 10.1016/j.fuel.2015.04.046.

[51] Z. Ilham, Z. Lubes, M. Zakaria, B. Sciences, F. Science, and K. Lumpur, “Analysis of Parameters for Fatty Acid Methyl Esters Production from Refined Palm Oil for Use as Biodiesel in the Single- and Two-stage Processes,” vol. 17, pp. 5–9, 2009.

[52] M. B. Nurum Nabi, J. Einar Hustad, and D. Kannan, “FIRST GENERATION BIODIESEL PRODUCTION FROM NON EDIBLE VEGETABLE OIL AND ITS EFFECT ON DIESEL EMISSIONS,” in *Proceedings of the 4th BSME-ASME International Conference on Thermal Engineering*, Dhaka, Bangladesh, 2008, pp. 748–753.

[53] P. Chitra, P. Venkatachalam, and A. Sampathrajan, “Optimisation of experimental conditions for biodiesel production from alkali-catalysed transesterification of Jatropha curcus oil,” *Energy for Sustainable Development*, vol. 9, no. 3, pp. 13–18, 2005, doi: 10.1016/S0973-0826(08)60518-9.

[54] H. J. Berchmans and S. Hirata, “Biodiesel production from crude Jatropha curcas L. seed oil with a high content of free fatty acids,” *Bioresour Technol*, vol. 99, no. 6, pp. 1716–1721, 2008, doi: 10.1016/j.biortech.2007.03.051.

[55] N. C. Om Tapanes, D. A. Gomes Aranda, J. W. de Mesquita Carneiro, and O. A. Ceva Antunes, “Transesterification of Jatropha curcas oil glycerides: Theoretical and experimental studies of biodiesel reaction,” *Fuel*, vol. 87, no. 10–11, pp. 2286–2295, 2008, doi: 10.1016/j.fuel.2007.12.006.

[56] U. Rashid, F. Anwar, B. R. Moser, and S. Ashraf, “Production of sunflower oil methyl esters by optimized alkali-catalyzed methanolysis,” *Biomass Bioenergy*, vol. 32, no. 12, pp. 1202–1205, 2008, doi: 10.1016/j.biombioe.2008.03.001.

[57] D. Y. C. Leung and Y. Guo, “Transesterification of neat and used frying oil: Optimization for biodiesel production,” *Fuel Processing Technology*, vol. 87, no. 10, pp. 883–890, 2006, doi: 10.1016/j.fuproc.2006.06.003.

[58] P. Felizardo, M. J. Neiva Correia, I. Raposo, J. F. Mendes, R. Berkemeier, and J. M. Bordado, “Production of biodiesel from waste frying oils,” *Waste Management*, vol. 26, no. 5, pp. 487–494, 2006, doi: 10.1016/j.wasman.2005.02.025.

[59] M. C. Math and G. Irfan, “Optimization of restaurant waste oil methyl ester yield,” *J Sci Ind Res (India)*, vol. 66, no. 9, pp. 772–776, 2007.

[60] R. Chamola, M. F. Khan, A. Raj, M. Verma, and S. Jain, “Response surface methodology based optimization of in situ transesterification of dry algae with methanol, H2SO4 and NaOH,” *Fuel*, vol. 239, no. August 2018, pp. 511–520, 2019, doi: 10.1016/j.fuel.2018.11.038.

[61] M. Athar and S. Zaidi, “A review of the feedstocks, catalysts, and intensification techniques for sustainable biodiesel production,” *J Environ Chem Eng*, vol. 8, no. 6, p. 104523, 2020, doi: 10.1016/j.jece.2020.104523.

[62] O. Rachmaniah, Y.-H. Ju, S. Ramjan Vali, and I. Tjondronegoro, “A study on acid-catalyzed transesterification of crude rice bran oil for biodiesel production,” *Researchgate.Net*, no. March, 2004.

[63] S. H. Dhawane, B. Karmakar, S. Ghosh, and G. Halder, “Parametric optimisation of biodiesel synthesis from waste cooking oil via Taguchi approach,” *J Environ Chem Eng*, vol. 6, no. 4, pp. 3971–3980, 2018, doi: 10.1016/j.jece.2018.05.053.

[64] R. Banani, Y. Snoussi, M. Bezzarga, and M. Abderrabba, “Waste frying oil with high levels of free fatty acids as one of the prominent sources of biodiesel production,” *Journal of Materials and Environmental Science*, vol. 6, pp. 1178–1185, Jan. 2015.

[65] Y. Wang, S. Ou, P. Liu, F. Xue, and S. Tang, “Comparison of two different processes to synthesize biodiesel by waste cooking oil,” *J Mol Catal A Chem*, vol. 252, no. 1–2, pp. 107–112, 2006, doi: 10.1016/j.molcata.2006.02.047.

[66] G. R. Moradi, E. Arjmandzadeh, and R. Ghanei, “Single-Stage Biodiesel Production from Used Soybean Oil by using a Sulfuric-Acid Catalyst,” *Energy Technology*, vol. 1, no. 4, pp. 226–232, Apr. 2013, doi: https://doi.org/10.1002/ente.201200034.

[67] N. Saravanan, S. Puhan, G. Nagarajan, and N. Vedaraman, “An experimental comparison of transesterification process with different alcohols using acid catalysts,” *Biomass Bioenergy*, vol. 34, no. 7, pp. 999–1005, 2010, doi: 10.1016/j.biombioe.2010.02.008.

[68] S. V. Ghadge and H. Raheman, “Biodiesel production from mahua (Madhuca indica) oil having high free fatty acids,” *Biomass Bioenergy*, vol. 28, no. 6, pp. 601–605, 2005, doi: 10.1016/j.biombioe.2004.11.009.

[69] M. J. K. Bashir *et al.*, “Biodiesel fuel production from brown grease produced by wastewater treatment plant: Optimization of acid catalyzed reaction conditions,” *J Environ Chem Eng*, vol. 8, no. 4, p. 103848, 2020, doi: 10.1016/j.jece.2020.103848.

[70] X. Miao and Q. Wu, “Biodiesel production from heterotrophic microalgal oil,” *Bioresour Technol*, vol. 97, no. 6, pp. 841–846, 2006, doi: 10.1016/j.biortech.2005.04.008.

[71] L. F. Chuah, A. Bokhari, S. Yusup, J. J. Klemeš, B. Abdullah, and M. M. Akbar, “Optimisation and Kinetic Studies of Acid Esterification of High Free Fatty Acid Rubber Seed Oil,” *Arab J Sci Eng*, vol. 41, no. 7, pp. 2515–2526, 2016, doi: 10.1007/s13369-015-2014-1.

[72] A. S. Ramadhas, S. Jayaraj, and C. Muraleedharan, “Biodiesel production from high FFA rubber seed oil,” *Fuel*, vol. 84, no. 4, pp. 335–340, 2005, doi: 10.1016/j.fuel.2004.09.016.

[73] V. B. Veljković, S. H. Lakićević, O. S. Stamenković, Z. B. Todorović, and M. L. Lazić, “Biodiesel production from tobacco (Nicotiana tabacum L.) seed oil with a high content of free fatty acids,” *Fuel*, vol. 85, no. 17–18, pp. 2671–2675, 2006, doi: 10.1016/j.fuel.2006.04.015.

[74] B. Freedman, E. H. Pryde, and T. L. Mounts, “Variables affecting the yields of fatty esters from transesterified vegetable oils,” *J Am Oil Chem Soc*, vol. 61, no. 10, pp. 1638–1643, Oct. 1984, doi: https://doi.org/10.1007/BF02541649.

[75] S. M. P. Meneghetti *et al.*, “Biodiesel from Castor Oil: A Comparison of Ethanolysis versus Methanolysis,” *Energy & Fuels*, vol. 20, no. 5, pp. 2262–2265, Sep. 2006, doi: 10.1021/ef060118m.

[76] B. Karmakar, S. H. Dhawane, and G. Halder, “Optimization of biodiesel production from castor oil by Taguchi design,” *J Environ Chem Eng*, vol. 6, no. 2, pp. 2684–2695, 2018, doi: 10.1016/j.jece.2018.04.019.

[77] S. Halder, S. H. Dhawane, T. Kumar, and G. Halder, “Acid-catalyzed esterification of castor (Ricinus communis) oil: optimization through a central composite design approach,” *Biofuels*, vol. 6, no. 3–4, pp. 191–201, Jul. 2015, doi: 10.1080/17597269.2015.1078559.

[78] E. Quayson, J. Amoah, S. Hama, A. Kondo, and C. Ogino, “Immobilized lipases for biodiesel production: Current and future greening opportunities,” *Renewable and Sustainable Energy Reviews*, vol. 134, no. August, 2020, doi: 10.1016/j.rser.2020.110355.

[79] H. Fukuda, A. Kondo, and H. Noda, “Biodiesel fuel production by transesterification of oils,” *J Biosci Bioeng*, vol. 92, no. 5, pp. 405–416, 2001, doi: 10.1016/S1389-1723(01)80288-7.

[80] J. M. Marchetti, V. U. Miguel, and A. F. Errazu, “Possible methods for biodiesel production,” *Renewable and Sustainable Energy Reviews*, vol. 11, no. 6, pp. 1300–1311, 2007, doi: 10.1016/j.rser.2005.08.006.

[81] B. Zhang, Y. Weng, H. Xu, and Z. Mao, “Enzyme immobilization for biodiesel production,” *Appl Microbiol Biotechnol*, vol. 93, no. 1, pp. 61–70, 2012, doi: 10.1007/s00253-011-3672-x.

[82] Q. Li, J. Xu, W. Du, Y. Li, and D. Liu, “Ethanol as the acyl acceptor for biodiesel production,” *Renewable and Sustainable Energy Reviews*, vol. 25, pp. 742–748, 2013, doi: 10.1016/j.rser.2013.05.043.

[83] J. C. Naranjo, A. Córdoba, L. Giraldo, V. S. García, and J. C. Moreno-Piraján, “Lipase supported on granular activated carbon and activated carbon cloth as a catalyst in the synthesis of biodiesel fuel,” *J Mol Catal B Enzym*, vol. 66, no. 1–2, pp. 166–171, 2010, doi: 10.1016/j.molcatb.2010.05.002.

[84] X. Li *et al.*, “Enzymatic production of biodiesel from Pistacia chinensis bge seed oil using immobilized lipase,” *Fuel*, vol. 92, no. 1, pp. 89–93, 2012, doi: 10.1016/j.fuel.2011.06.048.

[85] M. Iso, B. Chen, M. Eguchi, T. Kudo, and S. Shrestha, “Production of biodiesel fuel from triglycerides and alcohol using immobilized lipase,” *J Mol Catal B Enzym*, vol. 16, no. 1, pp. 53–58, 2001, doi: 10.1016/S1381-1177(01)00045-5.

[86] F. Yagiz, D. Kazan, and A. N. Akin, “Biodiesel production from waste oils by using lipase immobilized on hydrotalcite and zeolites,” *Chemical Engineering Journal*, vol. 134, no. 1–3, pp. 262–267, 2007, doi: 10.1016/j.cej.2007.03.041.

[87] W. Du, Y. Y. Xu, D. H. Liu, and Z. B. Li, “Study on acyl migration in immobilized lipozyme TL-catalyzed transesterification of soybean oil for biodiesel production,” *J Mol Catal B Enzym*, vol. 37, no. 1–6, pp. 68–71, 2005, doi: 10.1016/j.molcatb.2005.09.008.

[88] S. V. Otari, S. K. S. Patel, V. C. Kalia, and J. K. Lee, “One-step hydrothermal synthesis of magnetic rice straw for effective lipase immobilization and its application in esterification reaction,” *Bioresour Technol*, vol. 302, no. January, p. 122887, 2020, doi: 10.1016/j.biortech.2020.122887.

[89] S. V. Otari, S. K. S. Patel, V. C. Kalia, and J. K. Lee, “One-step hydrothermal synthesis of magnetic rice straw for effective lipase immobilization and its application in esterification reaction,” *Bioresour Technol*, vol. 302, no. December 2019, p. 122887, 2020, doi: 10.1016/j.biortech.2020.122887.

[90] E. L. Regner, H. N. Salvatierra, M. D. Baigorí, and L. M. Pera, “Biomass-bound biocatalysts for biodiesel production: Tuning a lipolytic activity from Aspergillus niger MYA 135 by submerged fermentation using agro-industrial raw materials and waste products,” *Biomass Bioenergy*, vol. 120, no. October 2018, pp. 59–67, 2019, doi: 10.1016/j.biombioe.2018.11.005.

[91] P. Paitaid and A. H-Kittikun, “Magnetic Cross-Linked Enzyme Aggregates of Aspergillus oryzae ST11 Lipase Using Polyacrylonitrile Coated Magnetic

Nanoparticles for Biodiesel Production," *Appl Biochem Biotechnol*, vol. 190, no. 4, pp. 1319–1332, 2020, doi: 10.1007/s12010-019-03196-7.

[92] A. A. Mehde, W. A. Mehdi, O. Severgün, S. Çakar, and M. Özacar, "Lipase-based on starch material as a development matrix with magnetite cross-linked enzyme aggregates and its application," *Int J Biol Macromol*, vol. 120, pp. 1533–1543, 2018, doi: 10.1016/j.ijbiomac.2018.09.141.

[93] N. Khan, M. Maseet, and S. F. Basir, "Synthesis and characterization of biodiesel from waste cooking oil by lipase immobilized on genipin cross-linked chitosan beads: A green approach," *Int J Green Energy*, vol. 17, no. 1, pp. 84–93, 2020, doi: 10.1080/15435075.2019.1700122.

[94] D. Bresolin *et al.*, "Synthesis of a green polyurethane foam from a biopolyol obtained by enzymatic glycerolysis and its use for immobilization of lipase NS-40116," *Bioprocess Biosyst Eng*, vol. 42, no. 2, pp. 213–222, 2019, doi: 10.1007/s00449-018-2026-9.

[95] W. Jin, Y. Xu, and X. W. Yu, "Formation lipase cross-linked enzyme aggregates on octyl-modified mesocellular foams with oxidized sodium alginate," *Colloids Surf B Biointerfaces*, vol. 184, no. September, p. 110501, 2019, doi: 10.1016/j.colsurfb.2019.110501.

[96] S. Bano, A. S. Ganie, S. Sultana, S. Sabir, and M. Z. Khan, "Fabrication and Optimization of Nanocatalyst for Biodiesel Production: An Overview," *Front Energy Res*, vol. 8, no. December, 2020, doi: 10.3389/fenrg.2020.579014.

[97] S. A. Hosseini, "Nanocatalysts for biodiesel production," *Arabian Journal of Chemistry*, vol. 15, no. 10, 2022, doi: 10.1016/j.arabjc.2022.104152.

[98] K. Se, B. Honarvar, H. Esmaeili, and N. Esfandiari, "Enhanced biodiesel production from chicken fat using CaO / CuFe 2 O 4 nanocatalyst and its combination with diesel to improve fuel properties," vol. 235, no. August 2018, pp. 1238–1244, 2019, doi: 10.1016/j.fuel.2018.08.118.

[99] S. H. Teo *et al.*, "Efficient biodiesel production from Jatropha curcus using CaSO4/Fe2O3-SiO2 core-shell magnetic nanoparticles," *J Clean Prod*, vol. 208, pp. 816–826, 2019, doi: https://doi.org/10.1016/j.jclepro.2018.10.107.

[100] I. Ambat, V. Srivastava, E. Haapaniemi, and M. Sillanpää, "Nano-magnetic potassium impregnated ceria as catalyst for the biodiesel production," *Renew*

Energy, vol. 139, pp. 1428–1436, 2019, doi: https://doi.org/10.1016/j.renene.2019.03.042.

[101] M. Shi, P. Zhang, M. Fan, P. Jiang, and Y. Dong, “Influence of crystal of Fe2O3 in magnetism and activity of nanoparticle CaO@Fe2O3 for biodiesel production,” *Fuel*, vol. 197, pp. 343–347, 2017, doi: https://doi.org/10.1016/j.fuel.2017.02.060.

[102] K. Seffati, H. Esmaeili, B. Honarvar, and N. Esfandiari, “AC / CuFe 2 O 4 @ CaO as a novel nanocatalyst to produce biodiesel from chicken fat,” *Renew Energy*, vol. 147, pp. 25–34, 2020, doi: 10.1016/j.renene.2019.08.105.

[103] W. Xie, Y. Han, and H. Wang, “Magnetic Fe3O4/MCM-41 composite-supported sodium silicate as heterogeneous catalysts for biodiesel production,” *Renew Energy*, vol. 125, pp. 675–681, 2018, doi: https://doi.org/10.1016/j.renene.2018.03.010.

[104] Y. Liu, P. Zhang, M. Fan, and P. Jiang, “Biodiesel production from soybean oil catalyzed by magnetic nanoparticle MgFe2O4@CaO,” *Fuel*, vol. 164, pp. 314–321, 2016, doi: https://doi.org/10.1016/j.fuel.2015.10.008.

[105] P. Zhang, Q. Han, M. Fan, and P. Jiang, “Magnetic solid base catalyst CaO/CoFe2O4 for biodiesel production: Influence of basicity and wettability of the catalyst in catalytic performance,” *Appl Surf Sci*, vol. 317, pp. 1125–1130, 2014, doi: https://doi.org/10.1016/j.apsusc.2014.09.043.

[106] M. Feyzi, L. Nourozi, and M. Zakarianezhad, “Preparation and characterization of magnetic CsH2PW12O40/Fe–SiO2 nanocatalysts for biodiesel production,” *Mater Res Bull*, vol. 60, pp. 412–420, 2014, doi: https://doi.org/10.1016/j.materresbull.2014.09.005.

[107] M. Feyzi, A. Hassankhani, and H. R. Rafiee, “Preparation and characterization of Cs/Al/Fe3O4 nanocatalysts for biodiesel production,” *Energy Convers Manag*, vol. 71, pp. 62–68, 2013, doi: https://doi.org/10.1016/j.enconman.2013.03.022.

[108] M. A. Ali, I. A. Al-hydary, and T. A. Al-hattab, “Nano-Magnetic Catalyst CaO-Fe 3 O 4 for Biodiesel Production from Date Palm Seed Oil,” vol. 12, no. 3, pp. 460–468, 2017, doi: 10.9767/bcrec.12.3.923.460-468.

[109] Z. Salimi and S. A. Hosseini, “Study and optimization of conditions of biodiesel production from edible oils using ZnO/BiFeO3 nano magnetic catalyst,” *Fuel*, vol. 239, pp. 1204–1212, 2019, doi: https://doi.org/10.1016/j.fuel.2018.11.125.

[110] P. Zhang, M. Shi, M. Fan, P. Jiang, and Y. Dong, “Magnetic Solid Base Catalyst Fe3O4@Gly Used as Acid-Resistant Catalyst for Biodiesel Production,” *Journal of the Chinese Chemical Society*, vol. 65, no. 6, pp. 681–686, Jun. 2018, doi: https://doi.org/10.1002/jccs.201700368.

[111] S. Alaei, M. Haghighi, J. Toghiani, and B. Rahmani Vahid, “Magnetic and reusable MgO/MgFe2O4 nanocatalyst for biodiesel production from sunflower oil: Influence of fuel ratio in combustion synthesis on catalytic properties and performance,” *Ind Crops Prod*, vol. 117, pp. 322–332, 2018, doi: https://doi.org/10.1016/j.indcrop.2018.03.015.

[112] S. Tamjidi, H. Esmaeili, and B. Kamyab, “Performance of functionalized magnetic nanocatalysts and feedstocks on biodiesel production : A review study,” vol. 305, 2021.

[113] M. J. Borah, A. Devi, R. Borah, and D. Deka, “Synthesis and application of Co doped ZnO as heterogeneous nanocatalyst for biodiesel production from non-edible oil,” *Renew Energy*, vol. 133, pp. 512–519, 2019, doi: https://doi.org/10.1016/j.renene.2018.10.069.

[114] Y. Zhang, S. Niu, C. Lu, Z. Gong, and X. Hu, “Catalytic performance of NaAlO2/γ-Al2O3 as heterogeneous nanocatalyst for biodiesel production: Optimization using response surface methodology,” *Energy Convers Manag*, vol. 203, p. 112263, 2020, doi: https://doi.org/10.1016/j.enconman.2019.112263.

[115] G. Baskar, I. Aberna Ebenezer Selvakumari, and R. Aiswarya, “Biodiesel production from castor oil using heterogeneous Ni doped ZnO nanocatalyst,” *Bioresour Technol*, vol. 250, pp. 793–798, 2018, doi: https://doi.org/10.1016/j.biortech.2017.12.010.

[116] M. L. Ibrahim *et al.*, “Preparation of Na2O supported CNTs nanocatalyst for efficient biodiesel production from waste-oil,” *Energy Convers Manag*, vol. 205, p. 112445, 2020, doi: https://doi.org/10.1016/j.enconman.2019.112445.

[117] F. Qiu, Y. Li, D. Yang, X. Li, and P. Sun, “Heterogeneous solid base nanocatalyst: Preparation, characterization and application in biodiesel

production," *Bioresour Technol*, vol. 102, no. 5, pp. 4150–4156, 2011, doi: https://doi.org/10.1016/j.biortech.2010.12.071.

[118] X. Deng, Z. Fang, Y. Liu, and C.-L. Yu, "Production of biodiesel from Jatropha oil catalyzed by nanosized solid basic catalyst," *Energy*, vol. 36, no. 2, pp. 777–784, 2011, doi: https://doi.org/10.1016/j.energy.2010.12.043.

[119] M. Saeedi, R. Fazaeli, and H. Aliyan, "Nanostructured sodium–zeolite imidazolate framework (ZIF-8) doped with potassium by sol–gel processing for biodiesel production from soybean oil," *J Solgel Sci Technol*, vol. 77, no. 2, pp. 404–415, 2016, doi: 10.1007/s10971-015-3867-1.

[120] J. M. Fonseca, J. G. Teleken, V. de Cinque Almeida, and C. da Silva, "Biodiesel from waste frying oils: Methods of production and purification," *Energy Convers Manag*, vol. 184, no. January, pp. 205–218, 2019, doi: 10.1016/j.enconman.2019.01.061.

[121] I. Ambat, V. Srivastava, and M. Sillanpää, "Recent advancement in biodiesel production methodologies using various feedstock: A review," *Renewable and Sustainable Energy Reviews*, vol. 90, pp. 356–369, 2018, doi: https://doi.org/10.1016/j.rser.2018.03.069.

[122] M. Gayathiri, T. Pulingam, K. T. Lee, and K. Sudesh, "Activated carbon from biomass waste precursors: Factors affecting production and adsorption mechanism," *Chemosphere*, 2022.

[123] J. Wang and X. Guo, "Adsorption kinetic models: Physical meanings, applications, and solving methods," *J Hazard Mater*, vol. 390, p. 122156, 2020, doi: https://doi.org/10.1016/j.jhazmat.2020.122156.

[124] Forbes, "Produção de biodiesel do Brasil chegará a 10,2 bi de litros em 2025, diz StoneX," *Forbes*, 2022.

[125] A. Avinash and A. Murugesan, "Judicious Recycling of Biobased Adsorbents for Biodiesel Purification: A Critical Review," *Environ Prog Sustain Energy*, vol. 38, no. 3, p. e13077, May 2019, doi: https://doi.org/10.1002/ep.13077.

[126] M. G. Gomes, D. Q. Santos, L. C. de Morais, and D. Pasquini, "Purification of biodiesel by dry washing, employing starch and cellulose as natural adsorbents," *Fuel*, vol. 155, pp. 1–6, 2015, doi: https://doi.org/10.1016/j.fuel.2015.04.012.

[127] P. Ozpinar *et al.*, “Activated carbons prepared from hazelnut shell waste by phosphoric acid activation for supercapacitor electrode applications and comprehensive electrochemical analysis,” *Renew Energy*, vol. 189, pp. 535–548, 2022, doi: https://doi.org/10.1016/j.renene.2022.02.126.

[128] M. Li and R. Xiao, “Preparation of a dual Pore Structure Activated Carbon from Rice Husk Char as an Adsorbent for CO2 Capture,” *Fuel Processing Technology*, vol. 186, pp. 35–39, 2019, doi: https://doi.org/10.1016/j.fuproc.2018.12.015.

[129] S. M. Beyan, S. V. Prabhu, T. T. Sissay, and A. A. Getahun, “Sugarcane bagasse based activated carbon preparation and its adsorption efficacy on removal of BOD and COD from textile effluents: RSM based modeling, optimization and kinetic aspects,” *Bioresour Technol Rep*, vol. 14, p. 100664, 2021, doi: https://doi.org/10.1016/j.biteb.2021.100664.

[130] S. Wang, H. Nam, and H. Nam, “Preparation of activated carbon from peanut shell with KOH activation and its application for H2S adsorption in confined space,” *J Environ Chem Eng*, vol. 8, no. 2, p. 103683, 2020, doi: https://doi.org/10.1016/j.jece.2020.103683.

[131] X. Yang, D. Xie, W. Wang, S. Li, Z. Tang, and S. Dai, “An activated carbon from walnut shell for dynamic capture of high concentration gaseous iodine,” *Chemical Engineering Journal*, vol. 454, p. 140365, 2023, doi: https://doi.org/10.1016/j.cej.2022.140365.

[132] Q. Pu *et al.*, “Systematic study of dynamic CO2 adsorption on activated carbons derived from different biomass,” *J Alloys Compd*, vol. 887, p. 161406, 2021, doi: https://doi.org/10.1016/j.jallcom.2021.161406.

[133] J. Jjagwe, P. W. Olupot, E. Menya, and H. M. Kalibbala, “Synthesis and Application of Granular Activated Carbon from Biomass Waste Materials for Water Treatment: A Review,” *Journal of Bioresources and Bioproducts*, vol. 6, no. 4, pp. 292–322, 2021, doi: 10.1016/j.jobab.2021.03.003.

[134] Z. Heidarinejad, M. H. Dehghani, M. Heidari, G. Javedan, I. Ali, and M. Sillanpää, “Methods for preparation and activation of activated carbon: a review,” *Environ Chem Lett*, vol. 18, no. 2, pp. 393–415, 2020, doi: 10.1007/s10311-019-00955-0.

[135] S. A. Olawale, “Biosorption of Heavy Metals from Aqueous Solutions : An Insight and Review Archives of Industrial Engineering Review Article Biosorption of Heavy Metals from Aqueous Solutions : An Insight and Review Abstract :,” vol. 3, no. October, pp. 1–31, 2020.

[136] M. A. Al-Ghouti and D. A. Da’ana, “Guidelines for the use and interpretation of adsorption isotherm models: A review,” *Journal of Hazardous Materials*, vol. 393. Elsevier B.V., Jul. 05, 2020. doi: 10.1016/j.jhazmat.2020.122383.

[137] Y. Liu and Y. J. Liu, “Biosorption isotherms, kinetics and thermodynamics,” *Separation and Purification Technology*, vol. 61, no. 3. pp. 229–242, Jul. 15, 2008. doi: 10.1016/j.seppur.2007.10.002.

[138] C. J. Radkel, J. M. Prausnitz, J. Phys Chien, D. Boer, V. Ness, and I. C. Eng H E, “Adsorption of Organic Solutes from Dilute Aqueous Solution on Activated Carbon,” Publishers, 1972.

[139] Q. Hu, S. Ma, Z. He, H. Liu, and X. Pei, “A revisit on intraparticle diffusion models with analytical solutions: Underlying assumption, application scope and solving method,” *Journal of Water Process Engineering*, vol. 60, Apr. 2024, doi: 10.1016/j.jwpe.2024.105241.

[140] Y. S. Ho, D. A. J. Wase, and C. F. Forster, “Removal of lead ions from aqueous solution using sphagnum moss peat as absorbent,” *Water SA*, vol. 22, no. 3, pp. 219–224, 1996.

[141] F. Glasser, M. Doreau, A. Ferlay, and Y. Chilliard, “Technical note: Estimation of milk fatty acid yield from milk fat data,” *J Dairy Sci*, vol. 90, no. 5, pp. 2302–2304, 2007, doi: 10.3168/jds.2006-870.

[142] P. Bondioli and L. Della Bella, “An alternative spectrophotometric method for the determination of free glycerol in biodiesel,” *European Journal of Lipid Science and Technology*, vol. 107, no. 3, pp. 153–157, 2005, doi: 10.1002/ejlt.200401054.

[143] C. Morais De Almeida, “A produção e comercialização de noz em Portugal e no contexto mundial Walnut production and trade in Portugal and in the world context,” *Sociedade de Ciências Agrárias de Portugal*, 2020, doi: 10.19084/rca.19648.

[144] M. Chai, Q. Tu, M. Lu, and Y. J. Yang, “Esterification pretreatment of free fatty acid in biodiesel production, from laboratory to industry,” *Fuel Processing Technology*, vol. 125, pp. 106–113, 2014, doi: 10.1016/j.fuproc.2014.03.025.

[145] S. Froehner, J. Leithold, L. Fernando, and L. Júnior, “TRANSESTERIFICAÇÃO DE ÓLEOS VEGETAIS: CARACTERIZAÇÃO POR CROMATOGRAFIA EM CAMADA DELGADA E DENSIDADE,” 2016.

[146] M. Ashrafi, G. Bagherian, and N. Goudarzi, “Removal of Brilliant Green and Crystal violet from Mono-and Bi-component Aqueous Solutions Using NaOH-modified Walnut Shell,” 2018.

[147] S. Hajialigol and S. Masoum, “Optimization of biosorption potential of nano biomass derived from walnut shell for the removal of Malachite Green from liquids solution: Experimental design approaches,” *J Mol Liq*, vol. 286, Jul. 2019, doi: 10.1016/j.molliq.2019.110904.

[148] X. Li *et al.*, “Characterization and comparison of walnut shells-based activated carbons and their adsorptive properties,” *Adsorption Science and Technology*, vol. 38, no. 9–10, pp. 450–463, Dec. 2020, doi: 10.1177/0263617420946524.

[149] A. N. A. El-Hendawy, “Variation in the FTIR spectra of a biomass under impregnation, carbonization and oxidation conditions,” *J Anal Appl Pyrolysis*, vol. 75, no. 2, pp. 159–166, 2006, doi: 10.1016/j.jaap.2005.05.004.

[150] M. de Prá Andrade, D. Piazza, and M. Poletto, “Pecan nutshell: morphological, chemical and thermal characterization,” *Journal of Materials Research and Technology*, vol. 13, pp. 2229–2238, Jul. 2021, doi: 10.1016/j.jmrt.2021.05.106.

[151] Q. Yu, M. Li, X. Ji, Y. Qiu, Y. Zhu, and C. Leng, “Characterization and methanol adsorption of walnut-shell activated carbon prepared by KOH activation,” *Journal Wuhan University of Technology, Materials Science Edition*, vol. 31, no. 2, pp. 260–268, Apr. 2016, doi: 10.1007/s11595-016-1362-3.

[152] T. Bohli, A. Ouederni, N. Fiol, and I. Villaescusa, “Evaluation of an activated carbon from olive stones used as an adsorbent for heavy metal removal from aqueous phases,” *Comptes Rendus Chimie*, vol. 18, no. 1, pp. 88–99, 2015, doi: 10.1016/j.crci.2014.05.009.

[153] M. Doğan, M. Alkan, Ö. Demirbaş, Y. Özdemir, and C. Özmetin, “Adsorption kinetics of maxilon blue GRL onto sepiolite from aqueous solutions,” *Chemical Engineering Journal*, vol. 124, no. 1–3, pp. 89–101, Nov. 2006, doi: 10.1016/j.cej.2006.08.016.

[154] Z. Aksu, A. I. Tatli, and Ö. Tunç, “A comparative adsorption/biosorption study of Acid Blue 161: Effect of temperature on equilibrium and kinetic parameters,” *Chemical Engineering Journal*, vol. 142, no. 1, pp. 23–39, Aug. 2008, doi: 10.1016/j.cej.2007.11.005.

[155] J. Smith and H. Van Ness, *Chemical engineering kinetics*, Third ed. Singapore: McGraw Hill, 1987.

[156] Y. Chen, J. Tang, S. Wang, L. Zhang, and W. Sun, “Bimetallic coordination polymer for highly selective removal of Pb(II): Activation energy, isosteric heat of adsorption and adsorption mechanism,” *Chemical Engineering Journal*, vol. 425, Dec. 2021, doi: 10.1016/j.cej.2021.131474.

[157] S. Rovani, J. J. Santos, P. Corio, and D. A. Fungaro, “An alternative and simple method for the preparation of bare silica nanoparticles using sugarcane waste ash, an abundant and despised residue in the Brazilian industry,” *J Braz Chem Soc*, vol. 30, no. 7, pp. 1524–1533, 2019, doi: 10.21577/0103-5053.20190049.

APPENDIX A – CALIBRATION CURVE

Table A1. Calibration curve.

	Glycerol volume (mL)	Solvent Volume (mL)	Theorical concentration (mg/mL)	Abs
Curve 1	0.05	3.95	$2.01x10^{-4}$	0.006
	0.10	3.90	$4.02x10^{-4}$	0.016
	0.15	3.85	$6.03x10^{-4}$	0.031
	0.20	3.80	$8.03x10^{-4}$	0.043
	0.40	3.60	$1.61x10^{-3}$	0.075
	0.50	3.50	$2.01x10^{-3}$	0.095
	0.55	3.45	$2.21x10^{-3}$	0.103
	0.60	3.40	$2.41x10^{-3}$	0.112
	0.75	3.25	$3.01x10^{-3}$	0.127
Curve 2	0.80	3.20	$6.43x10^{-3}$	0.2225
	1.20	2.80	$9.64x10^{-3}$	0.4359
	1.60	2.40	$1.29x10^{-2}$	0.6097
	2.00	2.00	$1.61x10^{-2}$	0.8827
	2.40	1.60	$1.93x10^{-2}$	1.0275
	2.80	1.20	$2.25x10^{-2}$	1.2383
	3.20	0.80	$2.57x10^{-2}$	1.4726
	3.60	0.40	$2.89x10^{-2}$	1.6781
	4.00	0.00	$3.21x10^{-2}$	1.9068

Source: [2]

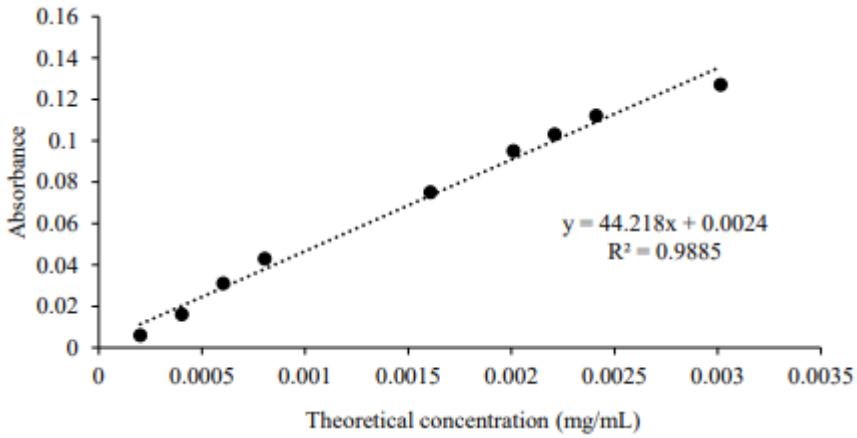

Figure A1. Calibration curve 1.

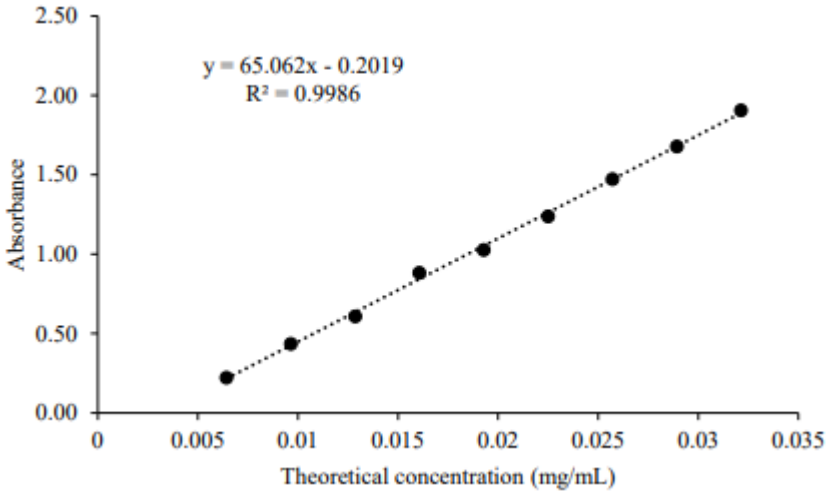

Figure A2. Calibration curve 2.

APPENDIX B – FAME IDENTIFICATION

Table B1. Gas chromatography FAME identification.

Elution Order	Peak name	Peak ID	Retention Time
1	Butyric acid methyl ester	C4:0	3.621
2	Caproic acid methyl ester	C6:0	4.953
3	Caprylic acid methyl ester	C8:0	6.25
4	Capric acid methyl ester	C10:0	7.416
5	Undecanoic acid methyl ester	C11:0	8.007
6	Lauric acid methyl ester	C12:0	8.629
7	Tridecanoic acid methyl ester	C13:0	9.31
8	Myristic acid methyl ester	C14:0	10.084
9	Myristoleic acd methyl ester	C14:1	10.427
10	Pentadecanoic acid methyl ester	C15:0	10.982
11	cis-10-Pentadecanoic acid methyl ester	C15:1	11.389
12	Palmitic acid methyl ester	C16:0	12.036
13	Palmitoleic acid methyl ester	C16:1	12.381
14	Heptadecanoic acid methyl ester	C17:0	13.263
15	cis-10-Heptadecanoic acid methyl ester	C17:1	13.662
16	Stearic acid methyl ester	C18:0	14.677
17, 18	Oleic acid methyl ester, Elaidic acid methyl ester	C18:1n9 (c+t)	15.033
19, 20	Linoleic acid methyl ester, Linolelaidic acid methyl ester	C18:2n6 (c+t)	15.784
21	gamma-Linolenic acid methyl ester	C18:3n6	16.315
22	alpha-Linolenic acid methyl ester	C18:3n3	16.891
23	Arachidic acid methyl ester	C20:0	18.068
24	cis-11-Eicosenoic acid methyl ester	C20:1n9	18.541
25	cis-11,14-Eicosadienoic acid methyl ester	C20:2	19.618
26, 30	cis-8,11,14-Eicosatrienoic acid methyl ester, Henicosanoic acid methyl ester	C20:3n6, C21:0	20.304
27	cis-11,14,17-Eicosatrienoic acid methyl ester	C20:3n3	20.92
28	Arachidonic acid methyl ester	C20:4n6	21.276
29	cis-5,8,11,14,17-Eicosapentaenoic acid methyl ester	C20:5n3	22.811
31	Behenic acid methyl ester	C22:0	23.08
32	Erucic acid methyl ester	C22:1n9	23.832
33	cis-13,16-Docosadienoic acid methyl ester	C22:2	25.582
34	cis-4,7,10,13,16,19-Docosahexanoic acid methyl ester	C22:6n3	25.989
35	Tricosanoic acid methyl ester	C23:0	26.629
36	Lignoceric acid methyl ester	C24:0	31.164
37	Nervonic acid methyl ester	C24:1n9	32.393

APPENDIX C – KINETICS PLOTS

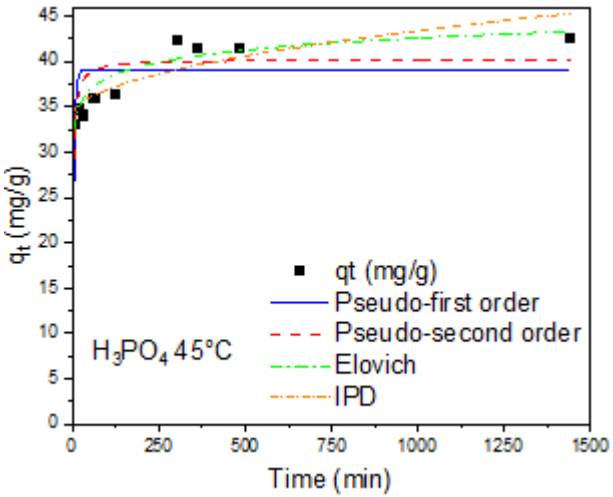

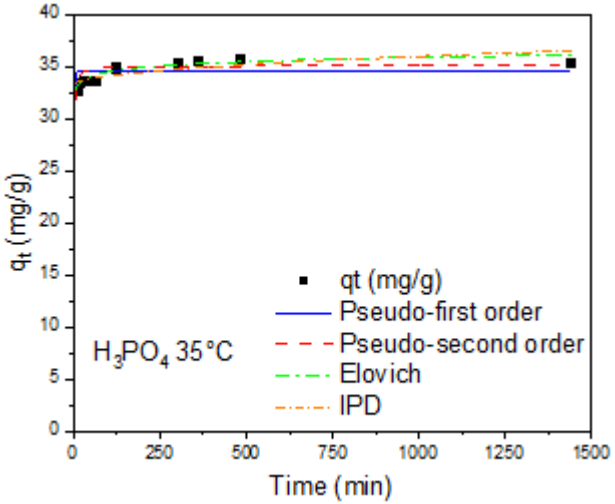

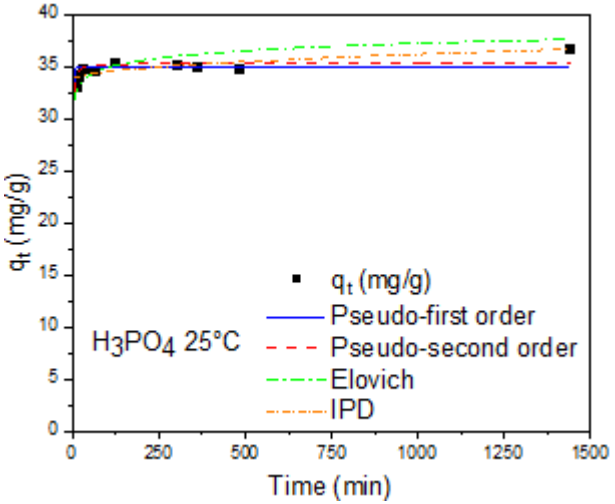

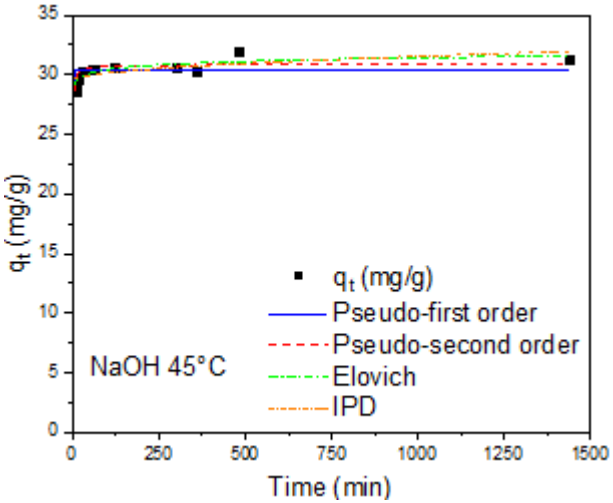

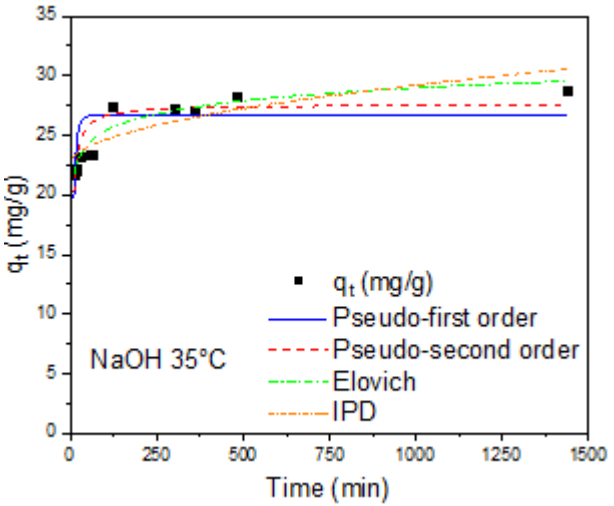

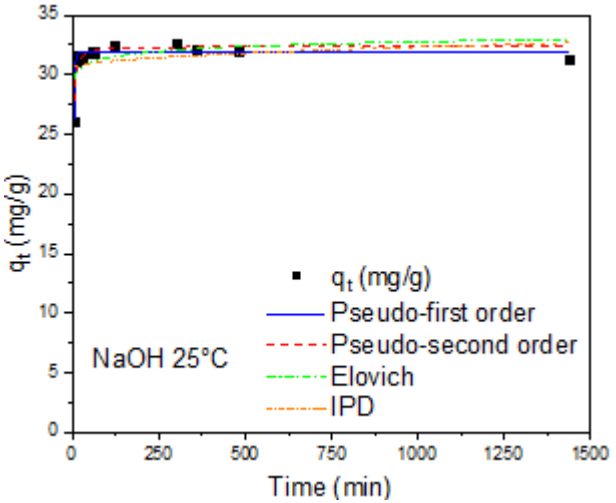

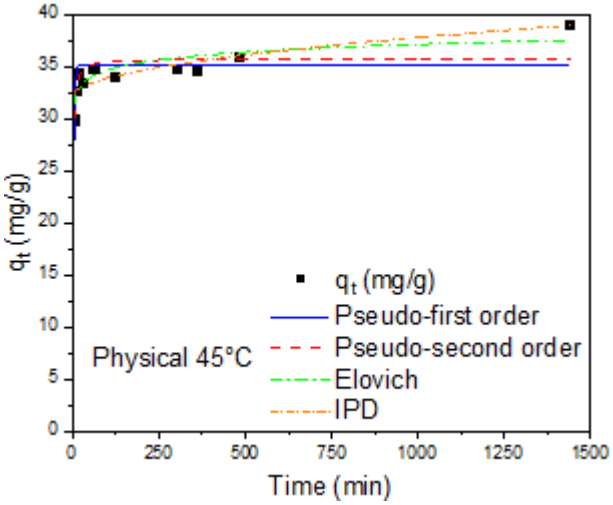
Physical 45°C
q_t (mg/g)
Pseudo-first order
Pseudo-second order
Elovich
IPD
q_t (mg/g)
Time (min)

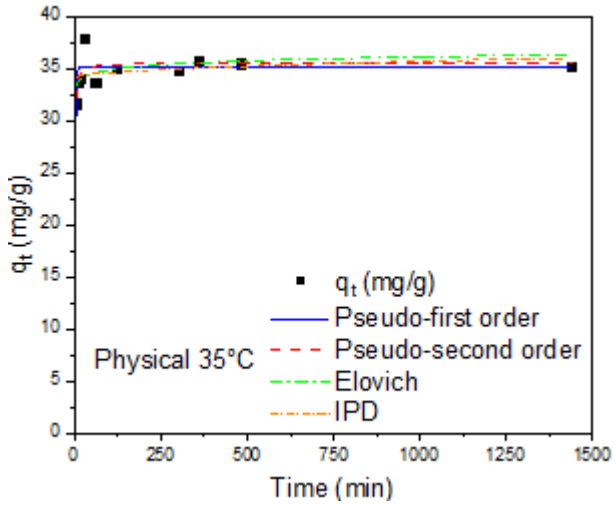
Physical 35°C
q_t (mg/g)
Pseudo-first order
Pseudo-second order
Elovich
IPD
q_t (mg/g)
Time (min)

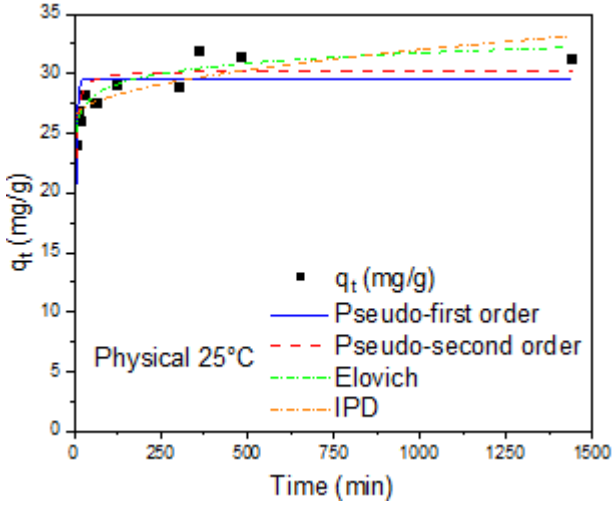
Physical 25°C
q_t (mg/g)
Pseudo-first order
Pseudo-second order
Elovich
IPD
q_t (mg/g)
Time (min)

APPENDIX D – PARTICIPATION IN A SCIENTIFIC CONFERENCE

CERTIFICADO DE PARTICIPAÇÃO

Por este meio certifica-se que

João Vitor Fabian

esteve presente no XXVII Encontro Luso Galego de Química organizado pela Delegação do Porto da SPQ e pelo Colégio Oficial de Químicos da Galiza (COLQUIGA), realizado na Fundação Dr. António Cupertino de Miranda, de 22 a 24 novembro 2023.

A Comissão Organizadora

Production of biodiesel from waste cooking oils and its purification using adsorption techniques with natural adsorbents

João Vitor Fabian[1,2,3] *, Miriam Domingues Guimarães[1,2], Camilla Groxko Smolich[1,2] Ticiane Sauer Pokriwieck[3], Ana Queiroz[1,2], António E. Ribeiro[1,2], Paulo Brito[1,2]

[1]Centro de Investigação de Montanha (CIMO), Instituto Politécnico de Bragança, Campus de Santa Apolónia, 5300-253 Bragança, Portugal
[2]Laboratório para a Sustentabilidade e Tecnologia em Regiões de Montanha, Instituto Politécnico de Bragança, Campus de Santa Apolónia, 5300-253 Bragança, Portugal
[3]Universidade Tecnológica Federal do Paraná, Linha Santa Bárbara, 85601-970, Francisco Beltrão, Brasil

joaofabian@alunos.utfpr.edu.br

The world's energy demands are steadily increasing each year, promoting the exploration of cleaner and more sustainable alternatives to classical fossil sources. In this context, biodiesel emerges as a promising candidate for replacing fossil diesel, making a significant contribution to carbon emissions reduction. One notable advantage lies in the ability to utilize waste cooking oils (WCO) as a feedstock for biodiesel production. This practice not only mitigates waste but also transforms a previously underutilized resource into a valuable source of renewable energy, thereby promoting sustainability and energy efficiency [1].

Currently, 95% of biodiesel production relies on first-hand feedstock due to its high conversion into fatty acid ethyl esters (FAEEs) or fatty acid methyl esters (FAMEs) [2]. However, this study introduces the utilization of Waste Cooking Oil (WCO) as a greener approach to biodiesel production. Biodiesel production can be achieved through alkaline catalyzed transesterification, with the aim of meeting the standards specified by EN 14214 at the end of its production process. Therefore, crude biodiesel obtained from the transesterification step needs to undergo glycerol purification in order to comply with the norm specification of a maximum free glycerin content of 0.02% (w/w). Hence, the present study seeks to produce and characterize activated carbons derived from walnut shells, and evaluate its use in the removal of glycerol from crude ethanolic biodiesel produced from WCO, a possible alternative to the traditional wet washing process, which results in the loss of between 0.2L to 10L of water per liter of biodiesel produced [3].

In this work, titration in triplicate was employed to determine the acid value of the oil, quantified as mg KOH/g of the sample, yielding a result of 0.8355±0.0274. This provided a preliminary assessment for the determination of the necessary alkaline catalyst percentage which would mitigate parallel saponification during the transesterification process. The reaction tests, executed in duplicate, included varying catalyst proportions of 0.5%, 0.6%, and 0.7% (w/w) relative to the processed oil. Gas chromatography (GC) was employed for the characterization of the produced biodiesel, revealing that a 0.5% (w/w) catalyst load was the optimal choice, providing a consistent average yield of 89.52% in FAEEs. Biodiesel production is currently conducted via the ethanol route with 1:7.5 oil/ethanol molar ratio, considering an excess in relation to the stoichiometric molar ratio 1:3 [4]. The research is also focused on the production of activated carbon materials, involving both chemical and physical activation techniques. Chemical activations will encompass the utilization of bases (KOH), acids (H_3PO_4), constituting a pivotal phase in enhancing the overall efficiency and sustainability of the biodiesel production process.

Acknowledgments

The authors are grateful to the Foundation for Science and Technology (FCT, Portugal) for financial support through national funds FCT/MCTES (PIDDAC) to CIMO (UIDB/00690/2020 and UIDP/00690/2020) and SusTEC (LA/P/0007/2021).

References

[1] X. Ma et al., Energy Conversion and Management, 229 (2021) 113760.
[2] S. Prasad et al., Bioresource Technology, 303 (2020) 122964.
[3] M. Catarino et al., Chemical Engineering Journal, 386 (2020) 123930.
[4] H. Hosseinzadeh-Bandbafha et al., Renewable and Sustainable Energy Reviews 161 (2022) 112411.